Eisosome organisation in the filamentous ascomycete *Aspergillus nidulans*

Ioannis Vangelatos[1], Katerina Roumelioti[1], Christos Gournas[1], Teresa Suarez[2], Claudio Scazzocchio[3,4] and Vicky Sophianopoulou[1*]

[1]Institute of Biology, National Center for Scientific Research, Demokritos (NCSRD), Athens, Greece

[2]Department of Cellular and Molecular Medicine, Centro de Investigaciones Biologicas (CSIC), 9, 28040 Madrid, Spain

[3]Department of Microbiology, Imperial College, London, UK

[4]Institut de Génétique et Microbiologie, Université Paris-Sud, UMR8621, Orsay, France

*For correspondence. Vicky Sophianopoulou, Institute of Biology, National Center for Scientific Research, Demokritos, Aghia Paraskevi 153 10, Athens, Greece, e-mail vicky@bio.demokritos.gr; Tel. (+30) 2106503602; Fax (+30) 2106511767.

Abstract

Eisosomes are sub-cortical organelles hitherto described only in *Saccharomyces cerevisiæ* as sites implicated in endocytosis. They comprise two homologue proteins, Pil1 and Lsp1, which colocalize with the transmembrane protein Sur7. These proteins are universally conserved in the ascomycetes. We identify in *Aspergillus nidulans* (and in all the Pezizomycotina) two homologues of Pil1/Lsp1, PilA and PilB, originating from a duplication independent from that extant in the Saccharomycotina. In the Aspergilli there are several Sur7-like proteins in each species, including one strict Sur7orthologue (SurG in *A. nidulans*). In *A. nidulans* conidiospores, but not in hyphæ, the three proteins colocalize at the cell cortex

and form tightly packed punctate structures that appear different from the clearly distinct eisosome patches observed in *S. cerevisiae*. These structures are assembled late during the maturation of conidia. In mycelia, punctate structures are present, but they are composed only of PilA, while PilB is diffused in the cytoplasm and SurG is located in vacuoles and endosomes. Deletion of each of the genes does not lead to any obvious growth phenotype, except for a moderate resistance to itraconazole. We could not find any obvious association between mycelial (PilA) eisosome-like structures and endocytosis. PilA and SurG are necessary for conidial eisosome organisation in ways that differ from their *S. cerevisiæ* homologues. These data illustrate that conservation of eisosomal proteins within the ascomycetes is accompanied by a striking functional divergence.

Introduction

In mammalian cells and in *S. cerevisiae* there is cogent evidence that membrane proteins are organised in discrete domains. In the latter organism, some transporters such as Can1p, Tat2p and Fur1p are organised in discrete domains on the plasma membrane. This specific domain has been named MCC for Membrane Compartment occupied by Can1p (Malinska *et al*., 2003, 2004; Grossman *et al*., 2007). As many as twenty-one proteins share the MCC localization pattern. These include MCC integral components such as the membrane protein Sur7 and the MCC-associated cytosolic proteins Pil1 and Lsp1 (see below, Grossman *et al*., 2008). Sur7 is a transmembrane protein consisting of four putative transmembrane domains and remains associated with the MCC compartments even under physiological conditions in which all other MCC components are dispersed (Grossman *et al*., 2007). The pair of homologous proteins Pil1 and Lsp1 are components of subcortical punctate assemblies named "eisosomes" (Walther *et al.,* 2006), which show identical localization to MCC proteins. Both MCC and eisosome components were shown to localize to furrow-like

invaginations of the plasma membrane (Strádalová *et al.,* 2009). The biological functions of MCC and eisosomes are quite elusive. They were initially characterised as sites of lipid and protein endocytosis (Walther *et al.,* 2006), but this function is by no means certain (Grossmann *et al.,* 2008). In *Candida albicans* Sur7 has additional roles in cell wall synthesis, actin cytoskeleton organisation and septin localization (Alvarez *et al.*, 2008 and 2009), while in *S. cerevisiae*, *sur7* mutants show a diminished efficiency of sporulation (Young *et al.,* 2002). Eisosomes are synthesised de novo in the bud during cell division (Moreira *et al.,* 2009). The Pil1/Lsp1 cytoplasmic components of the eisosome, together with the membrane protein Sur7 are conserved throughout the ascomycetes (Alvarez *et al.,* 2008, see below).

Recent work on eisosomal proteins has dealt mainly with two issues. Firstly, both Pil1 and Lsp1 are phosphorylated. Phosphorylation is mediated by a pair of redundant kinases, Pkh1p and Pkh2p. The evidence linking phosphorylation with eisosome assembly and disassembly is, however contradictory (Walther *et al.,* 2007; Luo *et al.,* 2008). The Pkh1/2 kinases are conserved throughout the eukaryotes and strictly conserved in the ascomycetes, one putative orthologue of the Pkh1/2 pair being present in all sequenced *Aspergillus* genomes. The second avenue of research is the identification of eisosomal associated proteins, including those necessary for eisosome assembly. Two recent reports have characterised a second conserved four transmembrane domain protein, Nce102p, as essential for eisosome assembly (Grossmann *et al.,* 2008, Strádalová *et al.,* 2009). The striking conservation, in all available ascomycete genomes, of proteins involved in eisosome structure or assembly posits an interesting paradox. No obvious macroscopic growth phenotype is seen in *S. cerevisiae* cells deleted for *PIL1*, *LSP1*, or *SUR7*, in single, double or triple mutants (Walther *et al.,* 2006). The only report dealing with eisosomal proteins in an organism other than *S. cerevisiae* concerns the Sur7 homologue of *Candida albicans*. CaSur7 is organised in punctate

eisosomal-like structures. At variance with *S. cerevisiae*, a deletion of the cognate gene results in a clear growth phenotype (see above), which resembles that resulting from the inhibition of β-glucan synthesis (Alvarez *et al.,* 2007).

Model filamentous ascomycetes such as *Neurospora crassa*, *Aspergillus nidulans*, *Sordaria macrospora* and *Podospora anserina*, together with a host of plant and animal pathogens and an increasing number of opportunistic human pathogens, belong to the sub-phylum Pezizomycotina, which may have diverged from the Saccharomycotina (such as *S. cerevisiae* and *C. albicans*) between 650 and more than 1000 million years ago (Padovan *et al.,* 2005). All these organisms are characterised by a highly polarised growth pattern, developmental processes which include the alternation of asexual and sexual cycles, involving two different types of spores, conidiospores and ascospores. Differently from the Saccharomycotina (see below), the sexual cycle involves a dicaryotic stage and a transient diploid, which never divides as such, but enters meiosis as soon as it is formed (Zickler, 2006 and refs. therein).

A. nidulans is arguably, among the Pezizomycotina, the organism where membrane proteins and endocytosis have been better studied. In this organism, a number of transporters, driven by their physiological promoters have been visualised in the cell membrane (UapC, Valdez-Taubas *et al.,* 2000; PrnB, Tavoularis *et al.,* 2001; UapA and AzgA, Pantazopoulou *et al.,* 2007; AgtA Apostolaki *et al.,* 2009; MstA, Forment *et al.,* 2006; FcyB, Vlanti *et al.,* 2008; UreA, M. Sanguinetti and A. Ramón, personal communication, FurD; G. Diallinas and F. Borbolis, personal communication). Load and chase experiments have shown that when the dye FM4-64 is endocytosed, it first appears in cortical punctate structures (Peñalva, 2005). The active research concerning membrane proteins (Diallinas 2007 for review), the determination and maintenance of polarity during development, including the possible involvement of sphingolipids (Li *et al.,* 2003), which may be involved in signalling eisosomal protein phosphorylation in *S. cerevisiæ*, and the ongoing recent work on

endocytosis (Peñalva, 2005; Sanchez-Ferrero and Peñalva, 2007; Araujo-Bazán *et al.*, 2008; Abenza *et al.*, 2009; Apostolaki *et al.,* 2009; Gournas *et al.,* 2010), makes *A. nidulans* an obvious model, within the Pezizomycotina to study eisosomal presence, structure and function. A description of the presence and fate of these organelles during asexual development is presented below.

Experimental procedures

Media and growth conditions

Minimal (MM) and complete (CM) media as well as growth conditions for *A. nidulans* were described by Cove (1966). pH 5.5 and 8.2 MM were made using MM without salt solution with the addition of 25mM and 25 mM Na_2HPO_4 respectively. Supplements were added when necessary at the adequate concentrations (http://www.gla.ac.uk/acad/ibls/molgen/aspergillus/supplement.html). Glucose 1% was used throughout as a carbon source. 5 mM urea or10 mM Ammonium L (+) tartrate were used as nitrogen sources. The antifungal drugs caspofungin (MSD, MERC and Co Inc. N.J. USA) and itraconazole (SIGMA) were used at final concentrations of 10 μg/ml and 15 μM respectively in CM. Caffeine, Calcofluor White, SDS, Congo Red and $CaCl_2$ were purchased from Sigma and used at final concentrations of 10 mM, 100 μg/ml, 50 μg/ml, 50 μg/ml and 100 mM respectively in CM (Hill *et al*., 2006). Staining with FM4-64 (Molecular Probes, Inc, USA) was according to Peñalva, 2005. In particular, cover slips with germinated conidia (12 h of growth at 25 °C) adhering to the glass surface were placed on top of plastic covers, covered with 0.1 ml of 10 μM FM4-64, incubated on ice for 15 min, washed in 5 ml MM and immediately observed. Vacuole staining with CMAC (7-amino-4-chloromethyl coumarin) (Molecular Probes, Inc, USA) was according to Tavoularis *et al.,* 2001. Cover slips with

germinated conidia were placed on top of plastic covers, covered with 0.1 ml of 1/1000 dilution of CMAC (5 mg/ml stock solution), incubated at 25 ºC for 30 min, washed twice with PBS, and observed under the phase contrast fluorescent microscope with the DAPI filter (Ex 365/10, DM 400, BA 400, UV-1A).

Crosses between *A. nidulans* strains were carried out as described by Pontecorvo *et al*., 1953. For growth tests, conidiospores were inoculated on solid CM or MM supplemented with the appropriate substrates and incubated at 25 °, 37 ° or 42 °C for 2-4 days. To monitor *PilA, PilB* and *SurG* mRNA steady state levels in different developmental stages from ungerminated conidia to young mycelia, strains were grown on liquid MM containing 1% glucose w/v and 5 mM urea as sole carbon and nitrogen sources respectively for 0, 4, 8, 12, 16 and 20 h at 25 ^{o}C.

Fungal and bacteria strains

***A. nidulans* strains:** The different auxotrophic mutations of *A. nidulans* strains are compiled by A.J. Clutterbuck (http://www.gla.ac.uk/acad/ibls/ molgen/aspergillus/index.html). In particular, *pantoB100, pabaA1, pabaB22, riboB2, pyroA4, pyrG89,* and *argB2* indicate auxotrophies for D-pantothenic acid, p-aminobenzoic acid, riboflavin, pyridoxine hydrochloride, uracil/uridine and L-arginine, respectively. The *nkuAΔ* mutation results in dramatically decreased frequency of heterologous integration events into the *A. nidulans* genome. The *LO1516* (see Table 1) strain expresses functional chimeric histone H1 molecules fused with the monomeric Red Fluorescence Protein (mRFP). The *VS125* (*agtA::sgfp*) strain expresses functional chimeric AgtA molecules fused with the Green Fluorescence Protein (sGFP). These markers do not affect the localization of eisosomal proteins. All strains used in this work are listed in Table 1. In every case MM indicates minimal media supplemented with the requirements relevant to the strains used in the

experiment. *pabaA1* was used as the wild type (wt) strain. The *VS79-81* and *VS83* strains (*pilA::sgfp, pilB::sgfp, surG::sgfp* and *pilA::mrfp* respectively, for complete genotypes see Table1) were isolated after transformation of protoplasts of the *nkuAΔ pyrG89 pyroA4* or *nkuAΔ pyrG89 riboB2* strain with the *pilA::sgfp::AfpyrG*$^+$, *pilB::sgfp::AfpyrG*$^+$, *surG::sgfp::AfpyrG*$^+$ or *pilA::mrfp::AfpyrG*$^+$ translational fusion cassettes (see below). *VS84-86* (*surGΔ::Afpyro*$^+$, *pilBΔ::AfpyrG*$^+$ and *pilAΔ::Afribo*$^+$ respectively) strains were isolated after transformation of protoplasts of *nkuAΔ pyrG89 pyroA4* or *nkuAΔ pyrG89 riboB2* recipient strain with the *surGΔ, pilBΔ* and and *pilAΔ* deletion cassettes (see deletion of the *pilA, pilB* and *surG* genes). The *VS87* (*pilAΔ::Afribo*$^+$ *pilBΔ::AfpyrG*$^+$) strain was isolated by crossing the *VS85* and *VS86* strains. The *VS91* (*pilA::mrfp pilB::sgfp*) and *VS94* (*pilA::mrfp surG::sgfp*) strains were isolated by crossing the *VS83* strain with the *VS80* and *VS81* strains respectively. The *VS128* (*pilB::sgfp pilAΔ::Afribo*$^+$) and *VS129* (*surG::sgfp pilAΔ::Afribo*$^+$) strains were isolated by crossing the *VS84* strain with the *VS80* and *VS81* strains respectively. The *VS118* (*pilA::mrfp surGΔ::Afpyro*$^+$) and *VS132* (*pilB::sgfp surGΔ::Afpyro*$^+$) strains were isolated by crossing the *VS84* strain with the *VS79* and *VS80* strains respectively. The *VS145* (*surG::sgfp hhoA::mrfp*) and *VS153* (*pilB::sgfp hhoA::mrfp*) strains were isolated by crossing the *LO1516* strain with the *VS80* and *VS81* strains respectively. The *VS172* (*agtA::sgfp pilAΔ::Afribo*$^+$) strain was isolated by crossing the *VS86* and *VS125* strains. The *VS186* strain was isolated by crossing the *VS83* strain with the TpA4 strain (Tavoularis *et al.,* 2001). The *nkuAΔ pyrG89 riboB2* and *nkuA pyrG89 pyroA4* strains were kindly provided by Dr. M. Peñalva and used for the deletion and the in locus fusions of the *pilA, pilB* and *surG* genes. For plasmid details see below and Table 2.

***Escherichia coli* strains:** The *E. coli* strain used was DH5A.

Transformation Methods: Transformation of *E. coli* was carried out as described by Sambrook (2001). Transformation of *A. nidulans* is described by Tilburn *et al.,* (1983).

Plasmids: The pRG3 plasmid carries the radish *18S rRNA* gene (Delcasso-Tremousaygue *et al*., 1988).The p1548 plasmid contains the *riboB* gene of *Aspergillus fumigatus* (Szewczyk *et al*., 2006), which complements the *riboB2* mutation of *A. nidulans* (kindly provided by Dr. M. Peñalva). The p1547 plasmid contains the *pyroA* gene of *A. fumigatus* (Szewczyk *et al*., 2006), which complements the *pyroA4* mutation of *A. nidulans* (kindly provided by Dr. M. Peñalva). The p1439 and p1491 plasmids contain a 5 Gly-Ala (5GA) linker fused in frame with the Green Fluorescent Protein (sGFP) and with the monomeric Red Fluorescent Protein (mRFP) respectively, followed by the *A. fumigatus pyrG* gene (Szewczyk *et al*., 2006, kindly provided by Dr. M. Peñalva).

DNA manipulations

Plasmid preparation from *E. coli* strains was carried out as described by Sambrook (2001). DNA digestion was carried out as described by Sambrook (2001). Total DNA extraction from *A. nidulans* is described by Lockington *et al*., (1985). Southern blot analysis was carried out according to Southern (1975) and Sambrook (2001). The restriction enzymes used to monitor the deletion of *pilA, pilB* or *surG* in the genome of *VS84, VS85* or *VS86* strains were *HindIII* (*pilAΔ::Afribo*$^{+}$ *surGΔ::Afpyro*$^{+}$) and *PstI* (*pilBΔ::AfpyrG*$^{+}$) respectively. *AfriboB*, *AfpyrG* and *AfpyroA* probes corresponding to the purified ~1 kb PCR fragments were obtained using as template DNA p1548, p1439 or p1547 plasmids respectively and PilAΔ (Ribo F-R), PilBΔ (PyrG F-R) or SurGΔ (Pyro F-R) primer pairs respectively (see Table 3).

High fidelity and long fragment PCR reactions were carried out using the kit Takara LA Taq^{TM} (Takara). High fidelity small fragment PCR reactions were carried out using Platinum Pfx polymerase (Invitrogen) while conventional PCR reactions were carried out using Taq polymerase (NEB). DNA bands were purified from agarose gels using the Wizard PCR preps DNA purification system (Promega). The ^{32}P-dCTP labelled DNA molecules, which were used as gene-specific probes, were prepared using the Megaprime^{TM} DNA labeling systems kit (Amersham LIFE SCIENCE).

Deletion of the *pilA, pilB* and *surG* genes

The entire *pilA, pilB* and *surG* open reading frames (1044 bp; ANID_05217.1, 1200 bp; ANID *3931.1 and 735* bp; ANID_4615.1 respectively) were replaced in an *nkuAΔ pyrG89 riboB2* (*pilA* and *pilB)* or *nkuAΔ pyroA4* (*surG*) strain by the *riboB* or *pyrG* or *pyroA (pilA, pilB* and *surG* respectively) genes after a double crossing over event, using the Fusion PCR gene replacement method (Szewczyk *et al*., 2006). The primers used are listed in Table 3. In the *pilA* deletion cassette, the fragment corresponding to the central part contains the *riboB* gene of *A. fumigatus* amplified from the p1548 plasmid using primers PilAΔ-Ribo F and PilAΔ-Ribo R. In the *pilB* deletion cassette, the fragment corresponding to the central part contains the *pyrG* gene of *A. fumigatus* amplified from p1439 plasmid using primers PilBΔ-PyrG F and PilBΔ-PyrG R. For the *surG* deletion cassette, the fragment corresponding to the central part contains the *pyroA* gene of *A. fumigatus* amplified from the p1547 plasmid using primers SurGΔ-Pyro F and SurGΔ-Pyro R. The sequences 1115 bp upstream and 1014 bp downstream the *pilA* ORF were amplified from genomic DNA of a wild type strain (*pabaA1*) using P1-P3 (PilAΔ) and P4-P6 (PilAΔ) primer pairs respectively. The sequences 1126 bp upstream and 1112 bp downstream the *pilB* ORF were amplified from genomic DNA of a wild type strain (*pabaA1*) using P1-P3 (PilBΔ) and P4-P6 (PilBΔ) primer pairs respectively.

The sequences 973 bp upstream and 1073 bp downstream the *surG* ORF were amplified from genomic DNA of a wild type strain (*pabaA1*) using P1-P3 (SurGΔ) and P4-P6 (SurGΔ) primer pairs respectively. The whole *pilA, pilB* and *surG* deletion cassettes, used to transform an *nkuAΔ pyrG89 riboB2* and *nkuAΔ pyroA4* strains, were amplified using P2 PilAΔ-P5 PilAΔ, P2 PilBΔ-P5 PilBΔ or P2 SurGΔ-P5 SurGΔ primer pairs respectively (see Table 3). Selection of transformants was carried out on urea containing minimal media lacking riboflavin or uracil/uridine or pyridoxine as required for each replacement. The *in locus* replacement of *pilA, pilB* and *surG* with *riboB, pyrG* and *pyroA* respectively was confirmed by Southern blot analysis (data not shown). The deleted outcrossed strains were checked by PCR using specific primer pairs: P2 PilAΔ - P5 PilA for *pilAΔ,* P2 PilBΔ - P6 PilB for *pilBΔ* and P2 SurGΔ- P5 SurG for *surGΔ* strains respectively (see Table 3).

Construction of the *pilA, pilB* and *surG in locus* fusions

Cassettes containing the *pilA::sgfp, pilB::sgfp, surG::sgfp*, *pilA::mrfp* and *pilB::mrfp* sequences were constructed by joining three different PCR fragments according to Szewczyk *et al*., (2006) using the PilA, PilB and SurG pairs of primers (see Table 3) respectively. To construct the *pilA::sgfp, pilB::sgfp, surG::sgfp*, *pilA::mrfp* and *pilB::mrfp* translational fusions, DNA fragments corresponding to the central part of the construction were amplified from p1439 and p1491 plasmids respectively. These fragments contain a 5 Gly-Ala (5GA) linker fused in frame with the sGFP and the mRFP proteins respectively, followed by the *pyrG* gene of *A. fumigatus.* The upstream flanking sequence of the *sgfp* and *mrfp* ORFs is a 1128 bp fragment containing a part of the *pilA* ORF followed by the 5GA linker while the downstream flanking sequence is a fragment containing a 1014 bp fragment corresponding to the 3' end of the *pilA* gene, just after the chain termination codon. The upstream flanking sequence of the *sgfp* ORFs is a fragment containing 1105 bp of the *pilB* ORF followed by the

5GA linker while the downstream flanking sequence is a fragment containing a 1112 bp fragment corresponding to the 3' downstream region of the *pilB* gene, just after the chain termination codon. The upstream flanking sequence of the *sgfp* ORFs is a 1157 bp fragment of the *surG* ORF followed by the 5GA linker while the downstream flanking sequence is a fragment containing a 1073 bp fragment corresponding to the 3' end of the *surG* gene, just following the chain termination codon. All fragments were amplified from genomic DNA of a wild type strain (*pabaA1*) using the P1-P3 (PilA, PilB or SurG) and P4 (PilA, PilB or SurG) primer pairs, respectively. The whole fusion cassettes were amplified using P2-P5 (PilA, PilB or SurG) pair of primers and were used to transform *nkuAΔ pyrG89 riboB2* (*pilA::sgfp, pilB::sgfp, surG::sgfp*, and *pilB::mrfp*) or *nkuAΔ pyroA4* (*pilA::mrfp*) strains. Transformants were selected on MM with urea as sole nitrogen source without uracil/uridine. The *in locus* replacement of *pilA, pilB* and *surG* with *pilA::sgfp, pilB::sgfp, surG::sgfp* or *pilA::mrfp* was confirmed by Southern blot analysis. Genomic DNA was restricted with *EcoRV* (*pilA::sgfp, pilA::mrfp*), *NcoI* (*pilB::sgfp*) or *PstI* (*surG::sgfp*) and hybridised with *AfriboB, AfpyrG* and *AfpyroA* sequence fragments respectively. These fragments were amplified from plasmids p1439, p1548 and p1547 using the primer pairs Ribo F-Ribo R, PyrG F-PyrG R and Pyro F-Pyro R respectively (see Tables 2 and 3). All transformants checked by Southern blot analysis contained single copy sequence integrations at the *pilA, pilB* and *surG* locus and they did not show any differences with the wild type controls under any of the conditions tested (see results).

RNA manipulations

Total RNA extraction from *A. nidulans* was carried out using the TRIzol® Reagent (Invitrogen) according to the manufacturer's instructions. RNA was separated on glyoxal agarose gels as described by Sambrook (2001). The hybridization technique is described by

Church and Gilbert (1984). To monitor RNA loading, the radish *18S rRNA* gene was used as probe (Delcasso-Tremousaygue *et al.,* 1988). This corresponds to the ~1.5 kb *EcoRI-EcoRI* fragment purified from plasmid pRG3. *pilA, pilB* and *surG* mRNA steady state levels were monitored by hybridizing with probes corresponding to the purified ~1 kb PCR fragments obtained using as template DNA from a wild type (*pabaA1*) strain and P1-P3 (PilA, PilB and SurG respectively) primer pairs.

Membrane protein extraction and western blot analysis

Protein extracts were prepared as in Kafasla *et al.,* 2007. In particular, mycelia grown for 16 h in MM containing 5 mM urea as sole nitrogen source and supplemented with the appropriate auxotrophies and conidiospores (0 h of growth) were harvested, frozen and ground in liquid nitrogen. All subsequent steps were carried at 4 ^{o}C. Conidia and mycelial powder was resuspended in 1.5 ml ice-cold extraction buffer (50 mM Tris-HCl, pH 7.4, 150 mM NaCl, 5 mM EDTA pH 8.0) supplemented with a protease inhibitor cocktail (Sigma) and 0.2 mM phenylmethanesulphonyl fluoride (PMSF). In conidia extraction buffer a volume of ~200 μl sterile glass beats (0.1mm) was added and the suspension was vortex for about 2 min. After 10 min incubation on ice, unbroken cells and larger cell debris were removed by low speed short centrifugation (3 min at 3.000 g). TCA was added to a final volume of 5%, followed by 10 min incubation on ice. Total proteins were precipitated by a 5 min centrifugation at 13000 g, washed with 500 μl Tris base and resuspended in extraction buffer. Sample protein concentration was measured by the method of Bradford. 20 μg protein samples were fractionated on a 10 % SDS-page gel and electroblotted (Mini PROTEAN$_{TM}$ Tetra Cell, BIO-RAD) onto a PVDF membrane (Macherey-Nagel) for immunodetection. The membrane was treated with 2 % non-fat dry milk and immunodetection was performed using a primary mouse anti-GFP monoclonal antibody (Roche) and a secondary goat anti-mouse

IgG HRP-linked antibody (Cell Signaling). Blots were developed by the chemiluminescent method using the ECL reagent (Amersham Bioscience).

Fluorescence microscopy (FM) and laser scanning confocal microscopy (LSCM)

10 ml of a suspension of 5 x 10^5 or 5 x 10^7 conidia / ml were inoculated onto sterile cover slips embedded into appropriate liquid culture media, were incubated for 4 h or 16 h at 25 ^oC and observed by FM and CSLM as previously described (Tavoularis *et al*., 2001; 2003). 200 µl of a suspension of 5 x 10^7 conidia / ml were inoculated into sterile Eppendorf tubes and observed by FM and CSLM as previously described. To elicit AgtA-GFP endocytosis, ammonium L(+) tartrate was added to a final concentration of 10 mM, 30, 60 and 120 min before observation as indicated in the legends to the figures. Filipin was used at a concentration of 25 µg / ml at 37 ^oC for 15 min before the observation. Samples were observed on an Axioplan Zeiss phase-contrast epifluorescent microscope with appropriate filters and the resulting images were acquired with a Zeiss-MRC5 digital camera using the AxioVs40 V4.40.0 software. Images were then processed in the Adobe Photoshop CS2 V9.0.2 software. Confocal scanning laser microscopy to examine PilA-sGFP, PilB-sGFP, SurG-sGFP, PilA-mRFP, PilB-mRFP and HhoA-mRFP localization was carried out on a BIO-RAD MRC 1024 CONFOCAL SYSTEM (Laser Sharp Version 3.2 Bio-Rad software, zoom ×2-5, excitation: 488 nm/Blue and 568 nm/Yellow (sGFP and mRFP respectively) samples at Laser Power 3 (PilA, SurG and HhoA) and 30% (PilB) respectively, Kalman filter N=5-6, 0.3 µm cut, iris: 7-8, crypton/argon laser, Nikon DIAPHOT 300 Microscope**,** ×60 (oil immersion) lens, emission filter 522/DF35. lens reference: Plan Apo 60/1.40 oil DM, Nikon Japan 160175, 60 DM/ Ph4, 160/0.17).

Bioinformatic tools and data bases

Data bases consulted were: http://www.fgsc.net/ through which most fungal genomes are accessible, specifically *Aspergillus* sequences were obtained through: http://www.broadinstitute.org/annotation/genome/aspergillus_group/MultiHome.html. The yeasts data bases consulted were http://www.genolevures.org/yeastgenomes.html, http://www.yeastgenome.org/, http://www.genedb.org/genedb/pombe/ and http://www.candidagenome.org/. The *Pneumocystis carinii* database is: http://pgp.cchmc.org/. Phylogenetic trees were constructed online using the different programs contained in http://www.phylogeny.fr/. Muscle alignments were carried out with http://www.ebi.ac.uk/Tools/muscle/index.html. T-Coffee alignments were carried at http://www.phylogeny.fr/. Alignments are shown with Boxshade http://www.ch.embnet.org/software/BOX_form.html. Transmembrane protein topologies were predicted with HMMTOP, http://www.enzim.hu/hmmtop/html/submit.html, PRED-TMR, http://athina.biol.uoa.gr/PRED-TMR2/input.html, TopPred, http://www.ch.embnet.org/software/TMPRED_form.html and SPLIT4 http://split.pmfst.hr/split/4/. Coiled coils were predicted with http://toolkit.tuebingen.mpg.de/pcoils and http://npsa-pbil.ibcp.fr/cgi-bin/npsa_automat.pl?page=npsa_lupas.html.

Results

Eisosomal core components in Aspergillus

A search on the available fungal data bases reveals that homologues of Pil1 and Lsp1 are present in all the ascomycetes (properly phylum Ascomycota). In the available genomes of

all the Pezizomycotina, including the Aspergilli, we found proteins belonging to two clades, that we shall call the PilA and the PilB clades. Very stringent conservation is seen within the PilA clade while the proteins of the PilB clade show a faster rate of divergence. Proteins of the PilA clade, show a central coiled-coil domain (residues 166-198 for PilA), similarly to Pil1 (Walther *et al.,* 2006) and Lsp1, while all proteins of the PilB clade show the presence of an additional carboxy-terminal coiled-coil domain (residues 147-178 and 225 to 244 for PilB, not shown). The PilA and PilB clades are represented in *A. nidulans* by ANID_05217.1 and ANID_03931.1 respectively. The duplication which generated PilA and PilB is possibly ancestral to the Pezizomycotina, as orthologues of ANID_05217.1 (73% identity) and ANID_03931.1 (56%identity) are present in *Tuber melanosporum* (Percudani, R. personal communication), a member of the Pezizales, a basal branch of the Pezizomycotina (Spatafora et *al.*, 2006). The PilA clade clusters with the Pil1-like Lsp1-like proteins of the Saccharomycotina, the latter arising from an independent duplication event at the root of the Saccharomycotina. For clarity's sake proteins from only two genomes (*S. cerevisiæ* and *Kluveromyces lactis*) of the later subphylum together with proteins from some representative genomes of the Pezizimycotina are shown in Fig. 1. A third duplication independent from those of the Saccharomycotina and Pezizomycotina, is present in all the available genomes of the genus *Schizosaccharomyces* represented in Fig. 1 by *S. pombe.* Two close homologues showing 64% to 42% identities respectively with the two *S. pombe* proteins are also present in *Pneumocystis carinii*, another member of the Taphrinomycotina (data not shown). The homologues present in the Taphrinomycotina are quite divergent from Pil1/PilA, but their position in the tree is consistent with the proposal that the ancestral "Pil protein" could have been Pil1/PilA like. This topology, indicating the occurrence of three independent duplications, one for each sub-phylum, is maintained when all available genomes are included in trees constructed with a variety of algorithms (our own unpublished data and

Olivera-Couto A. and Aguilar P., personal communication, Olivera-Couto, 2009). The meu14 protein of *S. pombe*, necessary for the second division of meiosis and the accurate formation of the forespore membrane (Ohtaka *et al.,* 2007), is clearly related to Pil1/Pil1A/Lsp1 (Okuzaki *et al.,* 2003, 22% identity with both Pil1 and PilA, 24% identity with PilB,). When included in trees similar to that shown in Fig. 1, it appears as an outgroup to both the Pil1/Lsp1/PilA (including the *S. pombe* putative eisosomal proteins) and to the PilB clades (our data not shown and Olivera-Couto, 2009).

The Sur7 transmembrane protein has been characterized as a component of eisosomes in both *S. cerevisiae* and *C. albicans* (see introduction). Three putative members of the Sur7 family of proteins are present in *A. nidulans*, ANID_04615.1, ANID_01331.1 and ANID_05213.1. These proteins represent each of the three clades of Sur7-like proteins present in the Aspergilli (Supplementary Figure 1) ANID_04615.1 (to be called SurG, cognate gene *surG*), is clearly the orthologue Sur7 proteins of *S. cerevisiae* and *C. albicans* (showing 21% and 27% identities respectively). The position of the four transmembrane domains, typical of Sur7, is conserved in the three homologues, together with the sequence showing similarities with Claudin-like domain (Alvarez *et al.,* 2008).

The sub-cellular localization of eisosomal proteins is developmentally regulated

To determine the subcellular localization of PilA, PilB and SurG we used strains carrying *pilA-gfp*, *pilA-mrfp, pilB-gfp* and *surG-gfp* alleles replacing the corresponding resident genes respectively. The GFP fusion strains behave like the wild type in relation to growth on complete media in the presence or absence of itraconazole (see below). It was also checked that the temporal pattern of expression of the mRNAs corresponding to each of the *gfp* fusion proteins is identical to that seen for the wild type genes from the wild type genes (not shown, see below).

Epifluorescence microscopy of ungerminated conidia (Fig. 2) showed PilA-GFP, PilB-GFP and SurG-GFP localized as patches in the periphery of the spores. SurG-GFP is additionally localized perinuclearly. The perinuclear location of SurG is more clearly shown by confocal microscopy in a strain carrying both SurG-GFP and the H1 histone gene fused to mRFP, suggesting a localization of SurG to the endoplasmic reticulum, similar to that shown by the ER chaperone ShrA (Fig. 2, panel B; Erpapazoglou *et al.,* 2006). Polar and equatorial sections of confocal microscopic images of ungerminated conidia showed that PilA-GFP patches are not as clearly separated as in *S. cerevisiae* (Supplementary Figure 2).

No change in the localization of PilA or PilB is seen during the period of isotropic growth. The same stands for the peripheral localization of SurG, nevertheless, the perinuclear ring disappears before the emergence of the germination tube (this is better seen in Fig. 9, see below). All three proteins are restricted to the periphery of the conidial head opposite to the emergent germ tube, while in young and older mycelia they have different destinations. PilA is present in discrete patches in young (16 h, Fig. 2) but also older and branching mycelia (20 and 24 h not shown). PilA spots in hyphae are not uniform in size and are not restricted to the periphery as they are in conidiospores. This is shown in Fig. 3, where the brightest PilA spots are localized at the periphery of the hyphae while smaller ones are present both at the interior of the hyphae and at its periphery. Furthermore, double-labelling of PrnB (the major proline transporter; Sophianopoulou and Scazzocchio, 1989; Tavoularis *et al.,* 2001) and PilA indicates that hyphal membrane bound PilA punctate structures (which we can equate to eisosomes) are localized to the internal face of the membrane (Fig. 3E). In hyphae, PilB-GFP is seen as very low intensity, diffused fluorescence in the cytoplasm (Fig. 3A), the settings of the microscope being such as to reflect faithfully the difference of fluorescence between the ungerminated conidia and the germlings. This suggests that the protein is down-regulated after germination. PilB-GFP is excluded from nuclei as shown in a strain carrying both PilB-

GFP and the gene encoding the H1 histone fused to mRFP (Fig. 3 panel B). Finally, SurG-GFP is in hyphae confined to the vacuole and endosomes (black arrows Fig. 3A), (some residual signal can be seen in the membrane of the conidial head) and this is confirmed by CMAC staining (not shown).

Expression of the pilA, pilB and surG genes

The accumulation of the three eisosomal proteins in conidia led us to investigate whether this is correlated with transcription of the cognate genes, from resting conidia through young mycelia. The results presented in Figure 4A show that both *pilA* and *surG* mRNAs accumulate more in resting conidia compared to all time points of germination tested. At variance with this, *pilB* mRNA is abundant in resting conidia and is not detectable within the sensitivity of the Northern blot at 4 h, 8 h, 12 h and 16 h after the onset of germination. The transcription of the *pilB* homologue of *A. fumigatus*, Afu6g08320, is also clearly detected in dormant conidia, and barely detectable at the onset of germination (Lamarre *et al.*, 2008).

The fluorescence signal (Fig. 2) seen in germlings and mycelia for PilB (cytosolic) and SurG (vacuolar) could be due either to the presence of the intact fusion proteins, to degradation products conserving the proteins C-termini or simply to degradation resistant GFP accumulating respectively in the cytosol and vacuoles. Western blots (Fig. 4B) carried out on protein extracts of ungerminated conidia (0 h) or young mycelia (16 h) grown in the same conditions as those used to investigate intracellular localization, show that bands corresponding to full-length PilA-GFP and PilB-GFP are present in both conidia and mycelia, while bands corresponding to full-length SurG-GFP are present in conidia and faintly observed in mycelia. The slower migrating bands of PilA-GFP and PilB-GFP have approximate apparent molecular weights of 70 kDa and 80 kDa respectively (calculated MW 67 kDa and 71.5 kDa respectively). The PilA and PilB bands running just below them have

apparent MWs of 62 and 72 kDa respectively. We cannot conclude from these data if N-terminal proteolysis and/or other post-translational modifications are responsible for the presence of these additional electrophoretic species, together with those seen between 48 and 27 kDa of the protein marker. The apparent MW of SurG-GFP is about 48 kDa (calculated MW 54 kDa), a difference which is not surprising for a protein comprising a highly hydrophobic moiety. A band of apparent molecular weight of 27 kD corresponding to free GFP, is only seen in strains carrying the SurG-GFP fusion. This, together with the down-regulation of the full length SurG-GFP observed after 16 h of growth, demonstrate that the vacuolar fluorescence detected in mycelia of SurG-GFP strains (Fig. 2A) mostly derives from free GFP and degradation intermediates.

Eisosomal proteins assemble during conidiogenesis

The presence and colocalization (see below) of the three eisosomal proteins in ungerminated conidia led us to investigate their appearance during conidial development. Figure 5 shows that during conidiogenesis the three proteins are present in late, mature conidia (Fig. 5B and 5C for PilA-GFP, 5G for PilB-GFP and 5H for SurG-GFP). PilA spots can be detected in the stalk of the conidiophore, in the vesicle, in metulae and phialides (Fig. 5A). Differently from PilB and SurG, which are only seen in mature, older conidia on the conidiophore, the appearance of PilA in conidia budding from the phialides is quite variable from one conidiophore to the other and even within the same conidiophore. Figures 5D and 5F show two extremes in which none or almost all of the emerging conidia express PilA-GFP respectively, while the 5E micrograph show an intermediate situation, with only some of the budding conidia expressing PilA-GFP. Control strains which did not include any GFP fusion protein do not show any conidiophore or conidiospore fluorescence under the same observation conditions (not shown).

Colocalization of PilA, PilB and SurG in quiescent conidia

PilA, PilB and SurG are localized at the periphery of resting conidia. We thus investigated their colocalization. To this aim we constructed strains carrying PilA-mRFP and PilB-GFP or SurG-GFP. Figure 6 shows colocalization of PilA with PilB, and colocalization of PilA with SurG in the periphery of the conidia; while there is obviously no colocalization of PilA with the perinuclear fraction of SurG. PilB fluorescence intensity follows more consistently the peaks of PilA fluorescence than that of SurG. It can be seen from both Figs. 2 and 6 that the localization pattern of SurG is less discontinuous and punctate than that of PilA and PilB.

Phenotypic characterization of deleted mutants: growth phenotypes

We have constructed strains deleted for *pilA*, *pilB* and *surG* (see Experimental procedures). A strain deleted for both *pilA* and *pilB* was also constructed. No growth phenotype, at 25 °, 37 ° and 42 °C was seen for any of the deleted strains on either complete or minimal media supplemented with urea, ammonium or nitrate as sole nitrogen sources (data not shown). Moreover, conidia from deleted *pilA*, *pilB* or *surG* strains exhibited swelling and polarity establishment (time of germination tube appearance) indistinguishable from that of a wild type strain at 25 °, 37 ° and 42 °C. This was seen after incubation of conidia in minimal media supplemented with urea as sole nitrogen source for 2 h, 4 h and 6 h respectively in the above conditions and observation of differential interference contrast (DIC) images using a phase contrast fluorescent microscope (data not shown). As eisosomal proteins are localized in quiescent conidia, we investigated whether they are important for conidial survival. The latter is not significantly different from the wild type in strains deleted for *pilA*, *pilB* or *surG* after incubation of freshly harvested conidia for 4 h at 4 °C (<100%), 25 °C (<60-70%), and

45 °C (<60-75%). Deleted strains were checked for sensitivity to caffeine, ethanol, SDS, Congo Red, $CaCl_2$ and the antifungal drugs caspofungin and itraconazole. Figure 7 shows that *pilAΔ, pilAΔpilBΔ* double mutants and *surGΔ*, but not *pilBΔ* strains show resistance to 15 μM itraconazole when compared to the wild type strain. The itraconazole resistance phenotype co-segregates in crosses with the genetic markers *riboB* and *pyroA* used to interrupt the *pilA* and *surG* genes respectively (see Materials and methods; data not shown). No other phenotype of resistance or hypersensitivity was observed.

Phenotypic characterization of deleted mutants: cell localization patterns and processes

PilA (but not PilB or SurG) is present in punctate structures in mycelia. The presence of ammonium results in endocytosis in germlings and mycelia of a number of transporters involved in the utilisation of nitrogen sources (Valdez-Taubas *et al.,* 2004; Pantazopoulou *et al.*, 2007; Apostolaki *et al.,* 2009). We have investigated whether the ammonium elicited endocytosis of the di-carboxylic amino acid transporter AgtA (Apostolaki *at al.,* 2009) was affected in a *pilA* deletion. The expression of AgtA is identical in $pilA^+$ and *pilAΔ* strains (not shown). The endocytosis of AgtA-GFP, checked at time intervals of 30, 60 and 120 min after addition of ammonium is identical in $pilA^+$ and *pilAΔ* strains, within the limits of the confocal microscope observation, being completed at 120 min in both strains (results not shown). Similarly, the rate of endocytosis of the lipophilic fluorochrome FM4-64 is no different, within the limits of the epifluorescence microscopic observation between a $pilA^+$ and a *pilAΔ* strain (not shown). Moreover, deletion of PilA does decrease neither the uptake of FM4-64 nor its early internalization pattern. As reported by Peñalva (2005) the earliest FM4-64 internalization intermediates are cortical punctuate structures. Figure 8 shows that these structures do not usually colocalize with PilA in germlings. Such colocalization as could be seen may well be coincidental. Thus, PilA foci are not obligatory endocytic portals

for this lipid marker as it has been proposed for eisosomes in *S. cerevisiae* (Walther *et al.,* 2006).

We have checked if any of the deleted strains is affected the distribution of filipin, a polyene antibiotic which selectively stains ergosterol and which can be detected by its blue fluorescence in UV light. No changes in filipin binding were seen in young mycelia of strains deleted for *pilA* and *surG* (data not shown). In these strains the strong filipin staining at the tip of the hypha is not altered. However, preliminary results strongly suggest that the distribution of filipin staining is affected in ungerminated conidia by the deletion of either *pilA* or *surG*, but not by the deletion of *pilB* (not shown).

Phenotypic characterization of deleted mutants: effects on eisosome assembly

We have checked the distribution of SurG-GFP and PilB-GFP in strains deleted for *pilA* and PilA-GFP and PilB-GFP in strains deleted for *surG*. Figure 9A shows that in *pilAΔ* ungerminated conidia (0 h), PilB-GFP patches become larger and more distinctly separated from each other. After 5 h of isotropic growth PilB is distributed in the cytoplasm as it is in the wild type, with less patches persisting at the conidial periphery. In a *pilAΔ* background, ungerminated conidia (0 h) show a significant decrease of SurG-GFP peripheral patches while the inner perinuclear ring remains intact indicating that PilA is required for proper localization of SurG at the conidial periphery. In the absence of SurG (Fig. 9B) the peripheral targeting and distribution of PilB-GFP is drastically affected, the protein being localized to a few bright clusters at the periphery of ungerminated conidia, which project into the cytoplasm, and to a diffuse cytoplasmic pool, which becomes more evident after 5 h of isotropic growth. At this time point PilB-GFP clusters are not only peripheral but appear also

in the cytoplasm. On the other hand deletion of SurG does not affect the localization of PilA-mRFP.

Discussion

Our own data (see supplementary data) and that of others (Olivera-Couto, A., and Aguilar, P., unpublished; Olivera-Couto, 2009) establish the universal presence of homologues of Pil1 and Lsp1 in the ascomycetes. The sequence divergence between the PilA and PilB clades of the Pezizomycotina, including differences in the conservation of putative phosphorylation sites (not shown), and the presence of a second coiled-coil domain in PilB, is associated, in *A. nidulans*, with a different fate in the course of development. While Pil1 and Lsp1 are integral components of eisosomes in all stages of the *S. cerevisiae* cell cycle, in *A. nidulans*, PilB shows colocalization with PilA only in conidia. The eisosomes of the *A. nidulans* conidiospore can be considered equivalent to those of *S. cerevisiae*, as they contain both Pil paralogues and SurG, the orthologue of Sur7 (see below). However, there are some intriguing differences between the *S. cerevisiae* cellular eisosomes and those of the conidiospores of *A. nidulans*. In *S. cerevisiae* there is about 1 eisosome / 3 μm^2 of surface area, well separated from each other at a distance >0.5 µm (Moreira *et al.*, 2009). In the *A. nidulans* conidiospore, eisosomes are more tightly packed; seem to touch each other and thus cannot be easily counted (Supplementary Figure 2). The peripheral localization of SurG does not match exactly the localization of PilA in conidia, but shows a more continuous distribution (Fig. 6). The perinuclear ring of SurG has not been reported for either *S. cerevisiae* or *C. albicans*.

In *S. cerevisiae*, Pil1 but not Lsp1 is essential for proper eisosome assembly (Walther *et al.,* 2007, Moreira *et al.,* 2009). In contrast to *S. cerevisiae*, in *A. nidulans,* the absence of PilA does not affect markedly the localization of its paralogue, PilB in conidia. In the absence of PilA, PilB patches are still uniformly distributed at the conidial periphery, but larger and

more widely spaced than in the wild type. In *S. cerevisiae*, Sur7 and Lsp1 are similarly affected by a *pil1* deletion. In *A. nidulans*, the distribution of SurG in a *pilAΔ* background (see Fig 10 and results section) is drastically altered, but the scanty SurG patches are very different from the large peripheral Sur7 clusters seen in *pil1* strains. A deletion of *SUR7* in *S. cerevisiae* has no effect on the localization of Pil1 and Lsp1. This applies also to strains deleted additionally for the two paralogues clustering with Sur7 in the phylogenetic tree (Supplementary Figure 1). Similar results were obtained for the deletion of Sur7 in *C. albicans* (Alvarez *et al.,* 2008). The situation is quite different in *A. nidulans*. While the distribution of PilA is not affected in *surGΔ* strains, that of PilB is affected drastically. The distribution of PilB in *surGΔ* strains is partly reminiscent, in quiescent conidia, of the distribution of Lsp1 in *pil1Δ* strains. That SurG is necessary for PilB localization is also consistent with the localization of PilB to the cytoplasm of wild type hyphae, where SurG is sequestered in the vacuole and endosomes and consequently may not be available to interact with PilB. Thus, the strong similarity of eisosomal components in *S. cerevisiae* cells and *A. nidulans* conidiospores is not correlated with identical interactions leading to their assembly.

Eisosomes have been defined as portals of endocytosis (Walther *et al.,* 2006). However, the data presented in this article implies that if they play a role in endocytosis in *A. nidulans*, this role is minor or limited to specific cargos, which remain unidentified. Neither the endocytosis of FM4-64 nor the ammonium-elicited endocytosis of the AgtA (di-carboxylic amino acid transporter, Apostolaki *et al.,* 2009 not shown) or PrnB (the major proline transporter, Sophianopoulou and Scazzocchio, 1989; not shown) are visibly affected in mycelia by a deletion of *pilA*, encoding the only eisosomal protein present in discrete foci in hyphae. It should be noted that although AgtA and PrnB proteins of *A. nidulans* and Hxt2 of *S. cerevisiae* are transporters with a homogeneous distribution in the plasma membrane, upon

endocytosis Hxt2 accumulates in discrete plasma membrane associated foci (Walther *et al.,* 2006), while the two *A. nidulans* proteins do not (Apostolaki *et al.,* 2009).

Endocytosis in *A. nidulans* has been investigated in mycelia (Peñalva, 2005), where is involved in the cycling of transporters (Valdez-Taubas, 2004; Pantazopoulou *et al.,* 2007; Apostolaki *et al.,* 2009; Gournas *et al.,* 2010) and in sensing external pH (Vincent *et al.,* 2003; Herranz *et al.,* 2005; Rodriguez-Galán *et al.,* 2009), but has not been investigated in the process of conidial germination, and the possibility remains open that the yeast-like eisosomes of conidiospores have a role in early, germination-related endocytosis events. The endocytic pathway is nearly-essential in *A. nidulans*. Deletion of components of ESCRT-III (Vps24, Rodriguez-Galán *et al.,* 2009, Vps20, Vps32, Vsp36, Calcagno-Pizzarelli, A.M. and Arst H.N., personal communication) results in a drastic impairment of growth. This contrasts with the absence of any obvious growth phenotype in *surGΔ*, *pilAΔ* and *pilBΔ* strains. A possible explanation of this apparent paradox is that, as proposed for *S. cerevisiae*, endocytosis could proceed by two independent pathways, one of which would not involve eisosomes (Grossmann *et al.,* 2008).

A vexing result, common to *S. cerevisiae* and *A. nidulans* is the absence of any drastic phenotype in deletion mutants of the eisosomal soluble (Pil1/Lsp1/PilA/PilB) or membrane proteins (Sur7/SurG). We did not observe any growth phenotype in any media or temperature tested for *pilA*, *pilB*, *pilA pilB* or *surG* deletions. Nevertheless it was reported at a recent meeting that a deletion of ANID_04615.1 (*surG*) results in growth impairment on minimal medium with nitrate as nitrogen source at 37 ° and 42 °C, an impairment that is only seen on complete medium at 42 °C (D. Chung and B. Shaw Abstract 322, 25th Fungal Genetics Meeting Asilomar, 2009, and personal communication). We did not observe this phenotype on minimal medium using a variety of nitrogen sources including nitrate, or on complete media at any temperature. The phenotype did not appear after outcrossing our deleted strain,

which eliminates the possibility that our strain could carry a suppressor of the growth phenotype. We do not know the reason for this difference, which merits investigation. However, a growth phenotype was observed for both *surG* and *pilA* deletions. This is the mild but clear resistance to itraconazole which co-segregates in crosses with each deletion. This is surprising, as deletions of *SUR7* in *Candida albicans*, result in marked hypersensitivity to fluconazole (Alvarez *et al.,* 2008), another triazole antifungal agent to which *Aspergillus* species are tolerant (Osherov *et al.,* 2001). Most probably this resistance operates at the level of conidial survival or germination and it may be in some way related with the miss- localization of filipin staining in conidia but not in mycelia, in both *surG* and *pilA* deletion strains. Triazole drugs act by inhibiting the cytochrome P450-dependent conversion of lanosterol to ergosterol. Filipin is a polyene macrolide antifungal agent that selectively binds and stains ergosterol at the plasma membrane.

One of the surprising results from this work is that, in *A. nidulans*, *S. cerevisiae*-like eisosomes assemble during conidial formation and disassemble during germination, resulting in germlings and mycelia in eisosome-like punctate structures comprising PilA and a novel cellular distribution (respectively cytosolic and vacuolar) for PilB and SurG. As no specific conidial survival phenotype was found in strain deleted for eisosomal components, this developmentally regulated distribution remains baffling. EglD, a putative endoglucanase comprising an expansin-like domain, also localizes at the periphery of ungerminated conidia (Bouzarelou *et al*., 2008). It would be of interest to study whether this localization implies a topological or functional association with eisosomes. In mycelia, PalI and PalH, involved in pH sensing, have been reported to form membrane-associated punctate structures (Calcagno Pizarelli *et al.*, 2007). The connection between PilA and these proteins is under investigation.

The work presented above is a first study of eisosomal structure and function in a model filamentous ascomycete. The universal presence of eisosomal proteins in the ascomycetes,

and probably in other fungal phyla (Alvarez *et al.,* 2008; Olivera-Couto, A., and Aguilar, P., unpublished; Olivera-Couto, 2009, Scazzocchio C., unpublished data) coupled with the paucity and diversity of the phenotypes of the deletion mutants observed in three different fungal species (*S. cerevisiae*, *C. albicans* and *A. nidulans*) and the striking developmental pattern of eisosomal proteins distribution seen in *A. nidulans* continues to be an unsolved paradox. The role of the Meu14 protein, a relative of the Pil1/PilA proteins in the meiosis of *S. pombe*, suggests that eisosomal proteins may have acquired entirely new functions in different ascomycete phylogenetic groups. Eisosomes, as defined in *S. cerevisiae* are present, within the asexual cycle, only in the conidia of *A. nidulans*, positing the question of their functional significance in this developmental stage. Punctate structures seen in mycelia can be considered to define a new class of assemblies comprising only one Pil paralogue. Thus it would be of interest to explore in this filamentous ascomycete the developmental fate of other conserved proteins known to share the *S. cerevisiae* MCC localization pattern.

Acknowledgements

We thank Dawoon Chung and Brian Shaw for open discussion relating to the phenotype found in their laboratory for a *surG* deletion, Pablo Aguilar and Agustina Olivera-Couto for sharing unpublished data and G. Diallinas for laboratory facilities. Specifically, CS wishes to thank AOC for very helpful insights concerning the phylogeny of the Pil-like proteins and Andrés Iriarte for help with interpretation of phylogenies. TS thank Miguel Peñalva for laboratory facilities, helpful discussions and encouragement at the onset of this work. The work of IV was in partial fulfillment of PhD thesis requirements at NCSRD. This work was supported by research grants from the NCSR “Demokritos” to IV and IKY to CG.

Figure legends

Figure 1

Eisosomal proteins in the Pezizomycotina. Phylogenetic unrooted tree including the Pil1 (YGR086C) and Lsp1 (YPL004C) proteins of *S. cerevisiae*, the two putative eisosomal proteins of second member of the Saccharomycotina, *Kluvermyces lactis* (KLLA); a member of the Taphrinomycotina, *S. pombe* (SPAC3C7.02c, SPCC736.15) and the PilA and PilB homologues (see text) of a number of representative fungi of the sub-phylum Pezizomycotina. The proteins of *A. nidulans* (Euriotiomycetes) are referred PilA as (ANID_05217.1) and PilB (ANID_03931.1) Other species are referred as: BC, *Botritis cynerea* (Leotiomycetes) CIGH *Coccidioides immitis* (Euriotiomycetes), MGG *Magnaporthe grisæ*, NCU, *Neurospora crassa* (Sordariomycetes) SNOG *Stegonospora nodorum* (Dothideomycetes) followed by their systematic numbers in the relevant databases. Alignments were carried out with T-Coffee, curated with the Phylogeny site internal curation programme (see Experimental procedures), the tree was obtained with the maximum likelihood program alLRT-PhyML (Anisimova and Gascuel, 2006, http://www.phylogeny.fr/version2_cgi/alacarte.cgi, 3) and re-drawn after a Drawtree image. The digits at the nodes represent aLRT (approximate likelihood ratio test) non-parametric branch support values (http://atgc.lirmm.fr/alrt/). The PilA clade is clustered with all the homologues of the Saccharomycotina (alTR=1), but note the weak support (0.25) of the node where the PilA clade branches out from the homologues in the Saccharomycotina; in trees (not shown) where many more species of Saccharomycotina and Pezizomycotina are included, the topology is maintained and the aLTR raises to >0. 80. For reasons of space we do not show the branch support aLTR values within the PilA clade, all nodes have strong support (aLRT>0.80) with the exception of the node where PilA branches out (aLRT=0.43).

While in this tree we show only representative species, the topology of a tight cluster of PilA homologues and a more loose cluster of PilB homologues is maintained in a tree constructed with the same or other algorithms and including at least one species of every genus of the Pezizomycotina for which there is an available sequence. Arrows show the nodes corresponding to the three independent duplications that gave origin to the PilA and PilB clades of the Pezizomycotina, the Pil1 and Lsp1 clades of the Saccharomycotina and the two clades of the Taphrinomycotina.

Figure 2

Subcellular localization of PilA, PilB and SurG proteins at various asexual developmental stages of the *A. nidulans* life cycle. (A) Representative pictures from epifluorescence microscopy of strains expressing chimeric PilA-GFP, PilB-GFP and SurG-GFP molecules in ungerminated (0 h), swollen (4 h) and germinated (8 h) conidia and young mycelia (12 h, 16 h). Strains were grown in the presence of 5 mM urea and 1% w/v glucose as sole nitrogen and carbon sources, at 25 ^{o}C. GFP fluorescence is shown on the upper panels of each row while Nomarski pictures of the same samples are shown on the lower panels. Black arrows indicate the central vacuole and endosomes. Bar 5 μm. (B) Representative pictures from laser scanning confocal microscopy of strains expressing both SurG-GFP and HhoA-mRFP (histone1-RFP) molecules in ungerminated wild type conidia (left panel) and both PilB-GFP and HhoA-mRFP molecules in young mycelia (16 h) (right panel). The strains were grown as in (A). Bar 5 μm

Figure 3

Panel A: Confocal z-stack sections showing PilA-GFP in a wild type strain. The strain was grown in the presence of 5 mM urea and 1% w/v glucose as sole nitrogen and carbon sources, for 16 h at 25 ^{o}C. Panels B, C and D: inverted black and white (b/w) fluorescence first z-stack section merged to the corresponding DIC. Bar 5 μm. Note that PilA spots are not uniform in size and are not restricted at the periphery of mycelia. The largest PilA eisosomes (filled arrows in Fig. 3D) are localized at the periphery while the smaller ones both at the interior and the periphery (dashed arrows). Panel E: Subcellular localization of PilA and PrnB proteins in mycelia. Representative pictures from laser scanning confocal microscopy of strains expressing both PilA-mGFP and PrnB-GFP molecules in young mycelia (12 h). The upper right inset in the "Merge" picture show a magnification of the boxed region. Strains were grown in the presence of 5 mM urea and 1% w/v glucose as sole nitrogen and carbon sources, at 25 ^{o}C. To induce *prnB* gene expression 20 mM of L-proline was added the last 2 h of growth (Tavoularis *et al.,* 2001). Bar 5 μm.

Figure 4

Panel A: Expression of the *pilA*, *pilB* and *surG* genes in a wild type strain. *pilA*, *pilB* and *surG* transcript levels in ungerminated (0 h), swollen (4 h) and germinated (8 h) conidia, young (12 h, 16 h) and older (20 h) mycelia. Strains were grown in the presence of 5 mM urea and 1% w/v glucose as sole nitrogen and carbon sources, at 25 ^{o}C. *18 S rRNA* steady-state levels are used to monitor the amount of RNA loading in each lane.

Panel B: Western blot analysis of the PilA, PilB, SurG tagged proteins. Approximately 20 μg of total protein fractions of conidia (0 h) and young mycelia (16 h) derived from strains expressing PilA-, PilB- or SurG-tag with GFP proteins, were fractionated on 10 % SDS-PAGE gel, transferred to a PVDF membrane and probed with a primary mouse anti-GFP

monoclonal antibody and a secondary goat anti-mouse IgG HRP-linked antibody. Protein markers are indicated on the right. Equal loading was checked by Comassie-blue staining.

Figure 5

Localization of PilA, PilB and SurG proteins during conidial development. Representative wide field fluorescence and DIC pictures of wild type conidiophores expressing chimeric PilA-GFP (**A**-**F**), PilB-GFP (**G**) and SurG-GFP (**H**) proteins are shown. The "Merge" section of panel A shows in inverted black and white an enlarged portion of the same conidial head shown in the PilA-GFP and DIC panels in order to highlight the PilA-GFP spots present in metulae and a budding phialide. Expression of PilB-GFP (**G**) and SurG-GFP (**H**) during conidial development is also presented. Young PilA-GFP expressing conidiophores are shown in **A** and **D**-**F** and mature in **B** and **C**. All strains were inoculated on microscope slides covered with MM containing 2% glycerol, 0.8% agarose and grown at 37 ^{o}C for two days. Bar 5 μm .

Figure 6

Colocalization of PilB with PilA and SurG with PilA in resting conidiospores. Representative confocal fluorescence micrographs (A-C and F-H) and fluorescence intensity profiles of PilA (red curve in E and J), PilB (green curve in E) and SurG (green curve in J) are shown. The fluorescence intensity, plotted along the yellow line in D (magnification of C) and I (magnification of H) that runs through both the inside and the periphery of the arrowed cell in C and H respectively, was calculated using the ImageJ software and normalised to the maximum value. Bar: 5 μm.

Figure 7

Itraconazole resistance of *pilAΔ, pilABΔ* and *surGΔ* strains. Cotton filtered *pilAΔ*, *pilBΔ*, *pilABΔ*, *surGΔ* and wild type conidiospore suspensions were prepared in PBS, counted using a Neubauer Counting Chamber to a concentration of ~10^6 conidia / ml and then plated (5 µl) as 10^{-1}, 10^{-2} and 10^{-3} serial dilutions on complete media (CM) in the absence or the presence of 15 µM itraconazole. The plates were grown at 37 °C for 3 days.

Figure 8

Representative epifluorescence (A-C) and confocal (D) images of a PilA-GFP strain labeled with FM4-64 Samples were taken after loading the dye on ice for 5 min (panel A). Note cortical punctate structures indicated by arrows: empty arrows indicate FM4-64 internalization sites free of PilA while filled arrows indicate FM4-64 internalization sites colocalizing with PilA.

Figure 9

Subcellular localization of PilB-GFP and SurG-GFP proteins expressed in conidia of a *pilAΔ* strain and of PilA-mRFP, PilB-GFP proteins expressed in conidia of a *surGΔ* strain. (A) Representative equatorial sections from laser scanning confocal microscopy of strains expressing chimeric PilB-GFP and SurG-GFP molecules in ungerminated (0 h) and swollen (5 h) conidia of a wild type and a *pilAΔ* strain. (B). Representative pictures from laser scanning confocal microscopy of strains expressing chimeric PilA-mGFP and PilB-GFP molecules in ungerminated (0 h) and swollen (5 h) conidia of a wild type and a *surGΔ* strain. In both (A) and (B) Nomarski pictures (DIC) of 0 h wild type conidia are shown. Bar 5 µM. Except for wt, PilA-GFP and PilB-GFP, two independent conidia are shown.

References

Abenza, J.F., Pantazopoulou, A., Rodríguez, J.M., Galindo, A., Peñalva, M.A. (2009) Long-distance movement of *Aspergillus nidulans* early endosomes on microtubule tracks. *Traffic* 10: 57-75.

Alvarez, F.J., Konopka, J.B. (2007) Identification of an N-acetylglucosamine transporter that mediates hyphal induction in *Candida albicans. Mol Biol Cell*. 18(3): 965-75.

Alvarez, F.J., Douglas, L.M., Rosebrock, A., Konopka, J.B. (2008) The Sur7 protein regulates plasma membrane organization and prevents intracellular cell wall growth in *Candida albicans*. *Mol Biol Cell* 19: 5214-25.

Alvarez, F.J., Douglas, L.M., Konopka, J.B. (2009) The Sur7 protein resides in punctate membrane subdomains and mediates spatial regulation of cell wall synthesis in *Candida albicans. Commun Integr Biol.* 2(2): 76-7.

Apostolaki, A., Erpapazoglou, Z., Harispe, L., Billini, M., Kafasla, P., Kizis, D., Peñalva, M.A., Scazzocchio, C., Sophianopoulou, V. (2009) AgtA, the dicarboxylic amino acid transporter of *Aspergillus nidulans*, is concertedly down-regulated by exquisite sensitivity to nitrogen metabolite repression and ammonium-elicited endocytosis. *Eukaryotic Cell*. 8(3): 339-52.

Araujo-Bazán, L., Peñalva, M.A., Espeso, E.A. (2008) Preferential localization of the endocytic internalization machinery to hyphal tips underlies polarization of the actin cytoskeleton in *Aspergillus nidulans*. *Mol Microbiol* 67(4): 891-905.

Bouzarelou, D., Billini, M., Roumelioti, K., Sophianopoulou, V. (2008). EglD, a putative endoglucanase, with an expansin like domain is localized in the conidial cell wall of *Aspergillus nidulans*. *Fungal Genet. Biol*. 45, 839–850.

Boylan, M.T., Mirabito, P.M., Willett, C.E., Zimmerman, C.R., Timberlake, W.E. (1987) Isolation and physical characterization of three essential conidiation genes from *Aspergillus nidulans. Mol Cell Biol.* 7(9):3113-8.

Church, G.M., Gilbert, W. (1984) Genomic sequencing. Proc *Natl Acad Sci U S A*. 81: 1991-5.

Calcagno-Pizarelli, AM., Negrete-Urtasun, S., Denison, S.H., Rudnicka, J.D., Bussink, H.J., Múnera-Huertas, T., Stanton, L., Hervás-Aguilar, A., Espeso, E.A., Tilburn, J., Arst, H.N. Jr., Peñalva, M.A. (2007) Establishment of the ambient pH signaling complex in Aspergillus nidulans: PalI assists plasma membrane localization of PalH. *Eukaryotic Cell*. 6(12): 2365-75.

Cove, D.J. (1966) The induction and repression of nitrate reductase in the fungus *Aspergillus nidulans*. *Biochim Biophys Acta* 113(1): 51-6.

Delcasso-Tremousaygue D, Grellet F, Panabieres F, Ananiev ED, Delseny M. (1988) Structural and transcriptional characterization of the external spacer of a ribosomal RNA nuclear gene from a higher plant. *Eur J Biochem*. 172(3): 767-76.

Forment J.V., Flipphi M., Ramon D., Ventura L., Maccabe A.P. (2006) Identification of the *mstE* gene encoding a glucose-inducible, low affinity glucose transporter in *Aspergillus nidulans*. *J Biol Chem*. 281:8339-46.

Diallinas, G. (2007). Aspergillus transporters. In "*The Aspergilli: Genomics, Medicine, Biotechnology and Research Methods*", eds. G. Goldman and S. Osmani, CRC press, pgs 301-310.

Erpapazoglou, Z., Kafasla, P., Sophianopoulou, V. (2006) The product of the SHR3 orthologue of *Aspergillus nidulans* has restricted range of amino acid transporter targets. *Fungal Genet. Biol.* 43: 222-233.

Fröhlich, F., Moreira, K., Aguilar, P.S., Hubner, N.C., Mann, M., Walter P., Walther, T.C. (2009) A genome-wide screen for genes affecting eisosomes reveals Nce102 function in sphingolipid signaling. *J Cell Biol*. 185(7): 1227-42.

Gournas C., Amillis S., Vlanti A., Diallinas G., (2010) Transport-dependent endocytosis and turnover of a uric acid-xanthine permease. *Mol Microbiol*. 75(1): 246-60.

Grossmann, G., Malinsky, J., Stahlschmidt, W., Loibl, M., Weig-Meckl, I., Frommer, W.B., Opekarová, M., Tanner W. (2008) Plasma membrane microdomains regulate turnover of transport proteins in yeast. *J Cell Biol*. 183(6): 1075-88.

Grossmann, G., Opekarová, M., Malinsky, J., Weig-Meckl, I., Tanner, W. (2007) Membrane potential governs lateral segregation of plasma membrane proteins and lipids in yeast. *EMBO J.* 26(1): 1-8.

Herranz, S., Rodríguez, J.M., Bussink, H.J., Sánchez-Ferrero, J.C., Arst, H.N. Jr., Peñalva, M.A., Vincent, O. (2005) Arrestin-related proteins mediate pH signaling in fungi. *Proc Natl Acad Sci U S A*. 102(34): 12141-6.

Hill, T.W., Loprete, D.M., Momany, M., Ha, Y., Harsch, L.M., Livesay, J.A., Mirchandani, A., Murdock, J.J., Vaughan, M.J., Watt, M.B. (2006) Isolation of cell wall mutants in Aspergillus nidulans by screening for hypersensitivity to Calcofluor White. *Mycologia* 98(3): 399-409.

Kafasla, P., Frillingos, S., and Sophianopoulou, V. (2007). The proline permease of *Aspergillus nidulans*: functional replacement of the native cysteine residues and properties of a Cysteine-less-transporter. *Fungal Genet. Biol.* 44 (7): 615-26.

Lamarre, C., Sokol, S., Debeaupuis, J.P., Henry, C., Lacroix, C., Glaser, P., Coppée, J.Y., François, J.M., Latgé, J.P. (2008) Transcriptomic analysis of the exit from dormancy of *Aspergillus fumigatus* conidia. *BMC Genomics* 16(9): 417.

Li, X.M., Momsen, M.M., Brockman, H.L., Brown, R.E. (2003) Sterol structure and sphingomyelin acyl chain length modulate lateral packing elasticity and detergent solubility in model membranes. *Biophys J.* 85(6): 3788-801.

Lockington, R.A., Sealy-Lewis, H.M., Scazzocchio, C., Davies, R.W. (1985) Cloning and characterization of the ethanol utilization regulon in *Aspergillus nidulans*. *Gene* 33(2): 137-49.

Luo, G., Gruhler, A., Liu, Y., Jensen, O.N., Dickson, R.C. (2008) The sphingolipid long-chain base-Pkh1/2-Ypk1/2 signaling pathway regulates eisosome assembly and turnover. *J Biol Chem.* 283(16): 10433-44.

Malínská, K., Malínský, J., Opekarová, M., Tanner, W. (2004) Distribution of Can1p into stable domains reflects lateral protein segregation within the plasma membrane of living *S. cerevisiae* cells. *J Cell Sci.* 117(Pt 25): 6031-41.

Malínská, K., Malínský, J., Opekarová, M., Tanner, W. (2003) Visualization of protein compartmentation within the plasma membrane of living yeast cells. *Mol Biol Cell* 14(11): 4427-36.

Moreira, K.E., Walther, T.C., Aguilar, P.S., Walter, P. (2009) Pil1 controls eisosome biogenesis. *Mol Biol Cell* 20(3): 809-18.

Okuzaki, D., Satake, W., Hirata, A., Nojima, H. (2003) Fission yeast *meu14+* is required for proper nuclear division and accurate forespore membrane formation during meiosis II. *J Cell Sci.* 116: 2721-35.

Oh, Y.T., Ahn, C.S., Kim, J.G., Ro, H.S., Lee, C.W., Kim, J.W. (2009) Proteomic analysis of early phase of conidia germination in *Aspergillus nidulans Fungal Genet Biol.* Nov 15. [Epub ahead of print].

Ohtaka, A., Okuzaki, D., Saito, T.T., Nojima, H. (2007) cp4, a meiotic coiled-coil protein, plays a role in F-actin positioning during *Schizosaccharomyces pombe meiosis*. *Eukaryotic Cell* 6(6): 971-83.

Olivera-Couto, A. (2009) Búsqueda de estructuras homólogas a los Eisosomas de *Saccharomyces cerevisiae* en eucariotas superiores. Tesis de Grado. Montevideo, Facultad de Ciencias, Universidad de la República.

Osherov, N., Kontoyiannis, D.P., Romans, A., May, G.S. (2001) Resistance to itraconazole in *Aspergillus nidulans* and *Aspergillus fumigatus* is conferred by extra copies of the *A. nidulans* P-450 14alpha-demethylase gene*, pdmA*. *J Antimicrob Chemother.* 48(1): 75-81.

Padovan, A.C., Sanson, G.F., Brunstein, A., Briones, M.R. (2005) Fungi evolution revisited: application of the penalized likelihood method to a Bayesian fungal phylogeny provides a new perspective on phylogenetic relationships and divergence dates of Ascomycota groups. *J Mol Evol*. 60(6): 726-35.

Pantazopoulou, A., Lemuh, N.D., Hatzinikolaou, D.G., Drevet, C., Cecchetto, G., Scazzocchio, C., Diallinas, G. (2007). Differential physiological and developmental expression of the UapA and AzgA purine transporters in *Aspergillus nidulans*. *Fungal Genet Biol* 44: 627-640.

Peñalva, M.A. (2005) Tracing the endocytic pathway of Aspergillus nidulans with FM4-64. *Fungal Genet Biol.* 42(12): 963-75.

Pontecorvo, G., Roper, J.A., Hemmons, L.M., MacDonald, K.D., Bufton, A.W (1953). The genetics of *Aspergillus nidulans*. *Adv. Genet*. 5(84): 141-238.

Rodríguez-Galán, O., Galindo, A., Hervás-Aguilar, A., Arst, H.N. Jr., Peñalva, M.A. (2009) Physiological involvement in pH signaling of Vps24-mediated recruitment of *Aspergillus* PalB cysteine protease to ESCRT-III. *J Biol Chem.* 284(7): 4404-12.

Sambrook, J., and Russell D. W. (2001) Molecular cloning: a laboratory manual, 3rd ed. Cold Spring Harbor Laboratory Press, Cold Spring Harbor, NY.

Sanchez-Ferrero, J.C., and Peñalva, MA. (2007) Endocytosis in: The Aspergilli: Genomics, Medical Applications, Biotechnology, and Research Methods. CRC Press, Osmani, S., and Goldman, G. editors.

Sophianopoulou, V., and Scazzocchio, C. (1989). The proline transport protein of *Aspergillus nidulans* is very similar to amino-acid transporters of *Saccharomyces cerevisiae. Mol. Microbiol.* 3(6): 705-714.

Spatafora, J.W., Sung, G.H., Johnson, D., Hesse, C., O'Rourke, B., Serdani, M., Spotts, R., Lutzoni, F., Hofstetter, V., Miadlikowska, J., Reeb, V., Gueidan, C., Fraker, E., Lumbsch, T., Lücking, R., Schmitt, I., Hosaka, K., Aptroot, A., Roux, C., Miller, A.N., Geiser, D.M., Hafellner, J., Hestmark, G., Arnold, A.E., Büdel, B., Rauhut, A., Hewitt, D., Untereiner, W.A., Cole, M.S., Scheidegger, C., Schultz, M., Sipman, H., Schoch, C.L. (2006) A five-gene phylogeny of Pezizomycotina. *Mycologia.* 98(6): 1018-28.

Strádalová, V., Stahlschmidt, W., Grossmann, G., Blazíková, M., Rachel. R., Tanner, W., Malinsky, J. (2009) Furrow-like invaginations of the yeast plasma membrane correspond to membrane compartment of Can1. *J Cell Sci*. 122: 2887-94.

Szewczyk, E., Nayak, T., Oakley, C.E., Edgerton, H., Xiong, Y., Taheri-Talesh, N., Osmani, S.A., Oakley, B.R. (2006) Fusion PCR and gene targeting in *Aspergillus nidulans*. *Nat Protoc*. 1(6): 3111-20.

Tavoularis, S., Scazzocchio, C., Sophianopoulou, V (2001). Functional expression and cellular localization of a green fluorescent protein-tagged proline transporter in *Aspergillus nidulans*. *Fungal Genet. Biol.* 33: 115–125.

Tavoularis, S.N., Tazebay, U.H., Diallinas, G., Sideridou, M., Rosa, A., Scazzocchio, C., Sophianopoulou, V. (2003). Mutational analysis of the major proline transporter (PrnB) of *Aspergillus nidulans*. *Mol Membr Biol*.20(4): 285-97.

Tilburn, J., Scazzocchio, C., Taylor, G.G., Zabicky-Zissman, J.H., Lockington, R.A., Davies, R.W. (1983) Transformation by integration in *Aspergillus nidulans*. Gene 26(2-3): 205-21.

Valdez-Taubas, J., Diallinas, G., Scazzocchio, C., Rosa, A.L. (2000) Protein expression and subcellular localization of the general purine transporter UapC from *Aspergillus nidulans.* *Fungal Genet Biol.* 30(2): 105-13.

Valdez-Taubas, J., Harispe, L., Scazzocchio, C., Gorfinkiel, L., Rosa, A.L. (2004) Ammonium-induced internalisation of UapC, the general purine permease from *Aspergillus nidulans. Fungal Genet Biol*. 41(1): 42-51.

Vincent, O., Rainbow, L., Tilburn, J., Arst, H.N. Jr., Peñalva, M.A. (2003) YPXL/I is a protein interaction motif recognized by *Aspergillus* PalA and its human homologue, AIP1/Alix. *Mol Cell Biol.* 23(5): 1647-55.

Vlanti, A., Diallinas, G. (2008) The *Aspergillus nidulans* FcyB cytosine-purine scavenger is highly expressed during germination and in reproductive compartments and is downregulated by endocytosis. *Mol Microbiol*. 68(4): 959-77.

Walther, T.C., Brickner, J.H., Aguilar, P.S., Bernales, S., Pantoja, C., Walter, P. (2006) Eisosomes mark static sites of endocytosis. *Nature* 439(7079): 998-1003.

Walther, T.C., Aguilar, P.S., Fröhlich, F., Chu, F., Moreira, K., Burlingame, A.L., Walter, P. (2007) Pkh-kinases control eisosome assembly and organization. *EMBO J*. 26(24): 4946-55.

Young, M.E., Karpova, T.S., Brügger, B., Moschenross, D.M., Wang, G.K., Schneiter, R., et al. (2002) The Sur7 family defines novel cortical domains in *Saccharomyces cerevisiae*, affects sphingolipid metabolism, and is involved in sporulation. *Mol Cell Biol.* 22(3): 927-34.

Zickler, D. (2006) Meiosis in Mycelial Fungi, in The Mycota I, Growth, Differentiation and Sexuality, Kües, U, and Fischer R., Eds. Springer-Verlag, Berlin, Heidelberg.

Zimmermann, C.R., Orr, W.C., Leclerc, R.F., Barnard, E.C., Timberlake, W.E. (1980) Molecular cloning and selection of genes regulated in *Aspergillus* development. *Cell* 21(3): 709-15.

Supplementary Figure 1

Sur7 homologues in the Aspergilli. A phylogenetic tree of homologues of Sur7 found in available genome sequences of the genus *Aspergillus*. Methods of tree-construction as in Fig. 1. All possible homologues of *S. pombe*, *S. cerevisiae* and *C. albicans* are also included. The possible homologues of a third member of the Saccharomycotina, phylogenetically distant from *S. cerevisiae*, *Yarrowia lipolytica* are included, as this inclusion results in a more robust tree. Functionally characterised genes (Sur7: YML025W; FMP45: YDL222C; CASur7: orf19.3414; SurG: ANID_04615.1) are indicated with the names reported in the literature, and shown in larger font, others by the accession number of the relevant data-bases. The

three physiologically characterised Sur7 orthologues are highlighted by grey rectangles. CA indicates *C. albicans*; Sur7, FMP45, YNL194C and YLR414C are the four Sur7 paralogues of *S. cerevisiae*, SPAC15A10.09c is the possible Sur7 homologue of *S. pombe*. YALI indicates homologues from *Yarrowia lipolytica*. Accession numbers starting with An corresponds to *A. niger*, Afu, *A. fumigatus*, ATG, *A. terreus*, AO, *A. oryzæ*, ACL *A. clavatus*, AFL *A. flavus*, ANID, *A. nidulans*, NFI, *N. fischeri*. For reasons of space only some aLRT non-parametric branch support values are shown, we have omitted those within tightly related groups. The crucial node separating where the Sur7/SurG clade branches from all other homologues has value of 1.00, which is indicated by a larger font within a grey frame. The three distinct tight clades found within the Aspergilli are highlighted by a grey background. After this tree was completed it come to our attention that *A. oryzæ* AO090005001554 has an exact orthologue in *A. flavus* (AFL2G_01448.2, 1000% identity).

Supplementary Figure 2

A: Comparison of Pil1 localization in *S. cerevisiae* cells (left panel adopted from Moreira *et al.,* 2009) and *A. nidulans* PilA localization in conidiospores (right panel) respectively.

B: Equatorial and polar confocal sections of ungerminated conidia. Panel I and II: inverted black/white confocal images resecting the equator and a pole respectively of three ungerminated conidia expressing PilA-GFP. Panel III and IV: ImageJ generated surface plots of fluorescence signal intensity of A and B respectively.

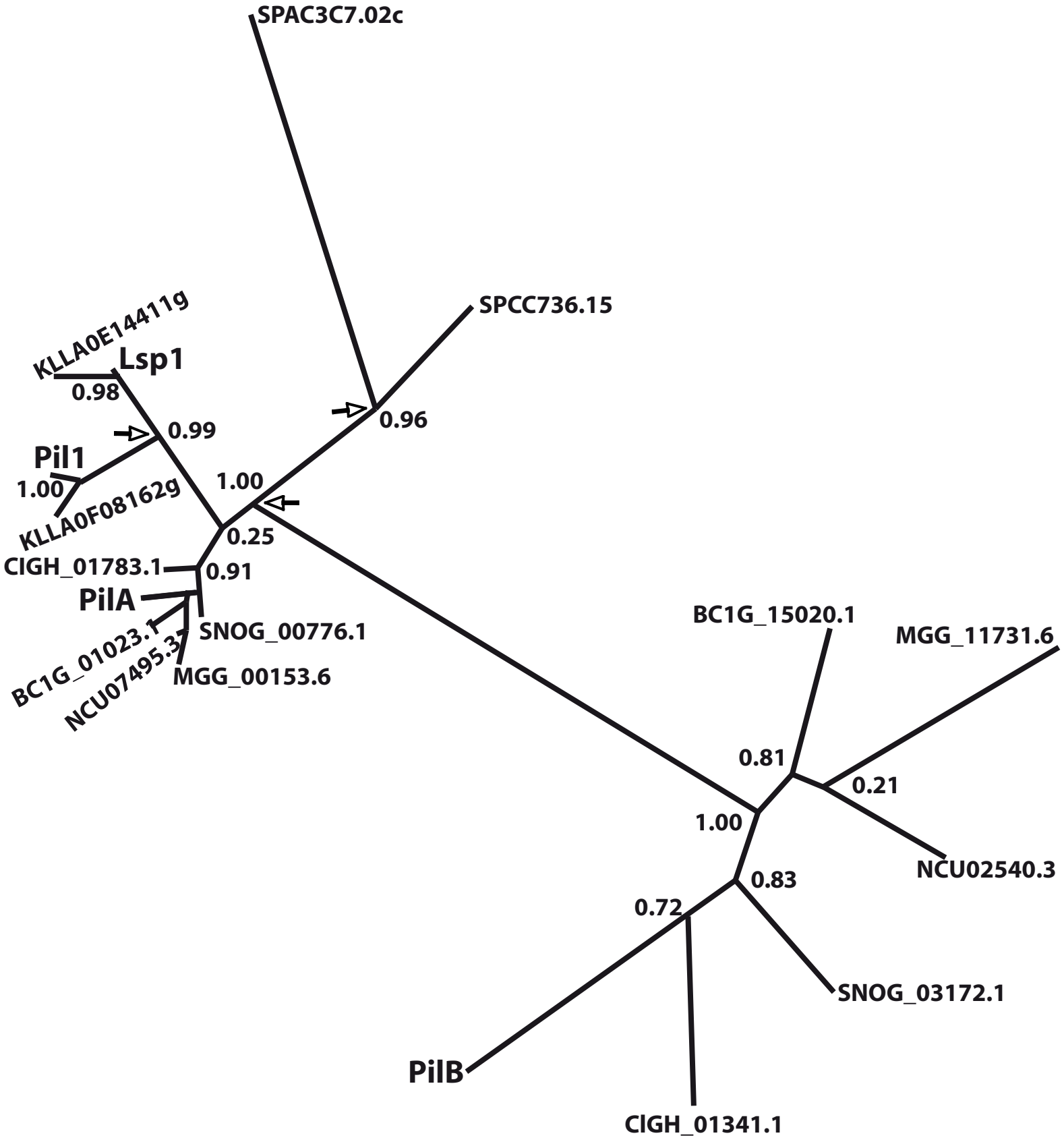
SPAC3C7.02c
SPCC736.15
KLLA0E14411g
Lsp1
0.98
0.99
0.96
Pil1
1.00
KLLA0F08162g
1.00
0.25
ClGH_01783.1
0.91
PilA
SNOG_00776.1
BC1G_01023.1
NCU07495.3
MGG_00153.6
BC1G_15020.1
MGG_11731.6
0.81
0.21
1.00
NCU02540.3
0.83
0.72
SNOG_03172.1
PilB
ClGH_01341.1

Figure 1

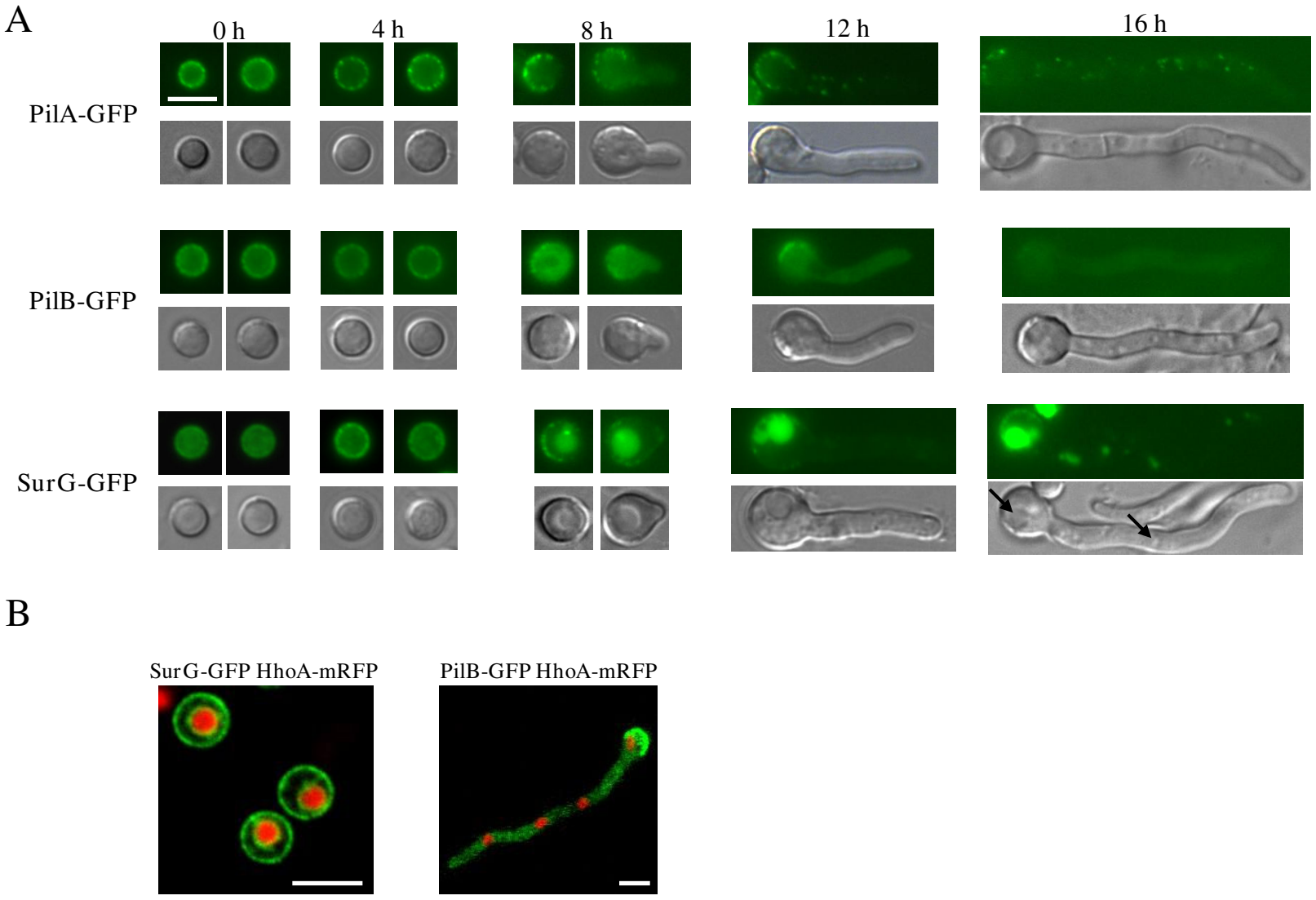
A
0 h
4 h
8 h
12 h
16 h
PilA-GFP
PilB-GFP
SurG-GFP
B
SurG-GFP HhoA-mRFP
PilB-GFP HhoA-mRFP

Figure 2

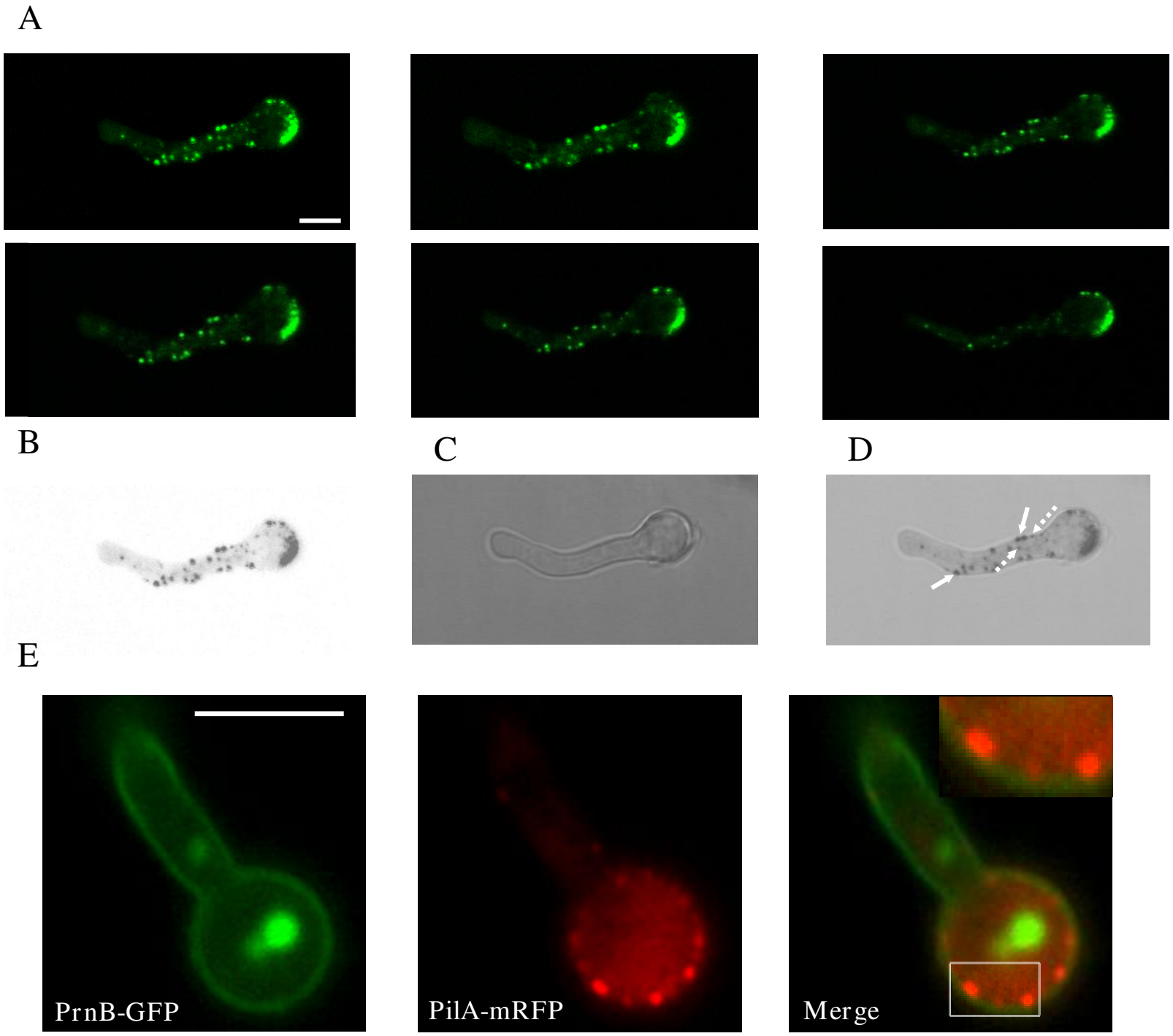

Figure 3

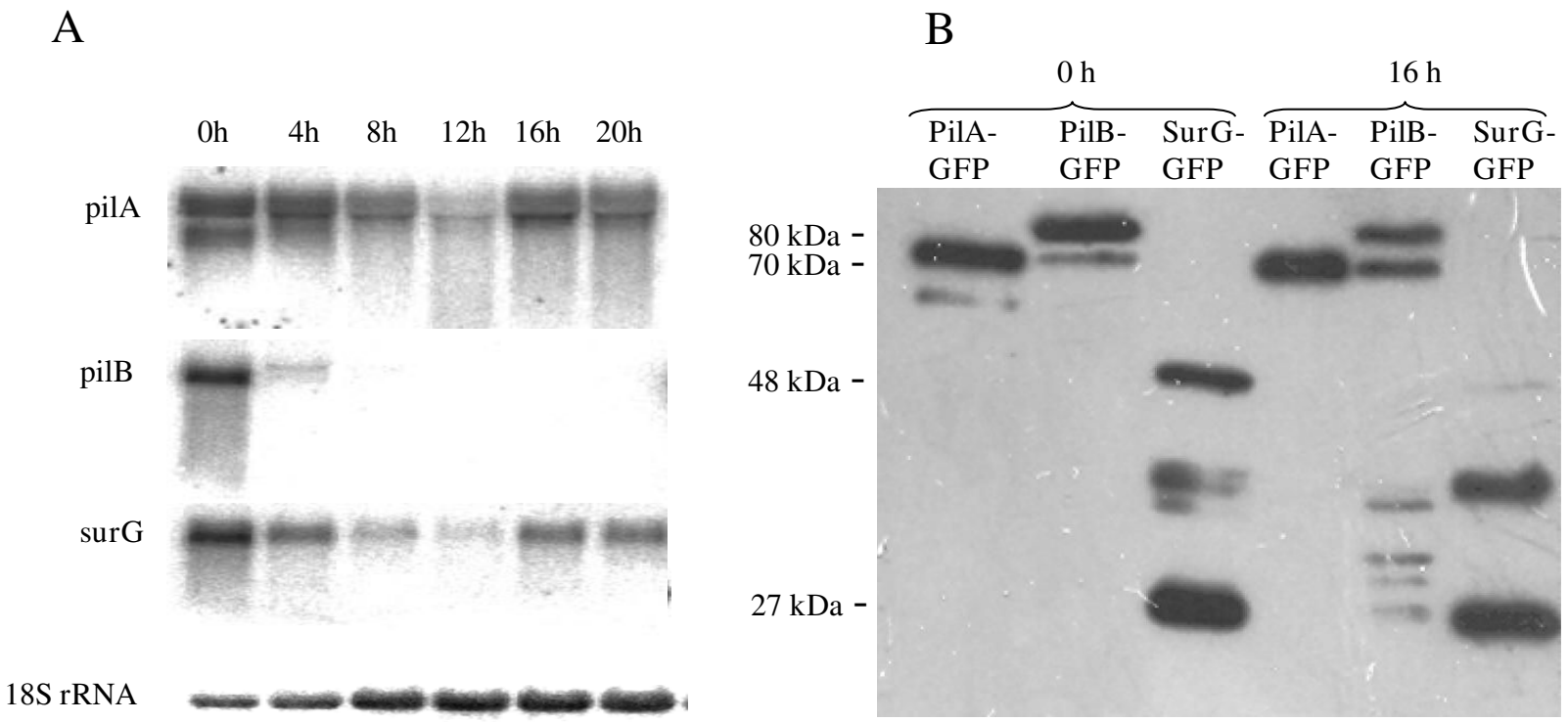
A
0h
4h
8h
12h
16h
20h
pilA
pilB
surG
18S rRNA
B
0 h
16 h
PilA-GFP
PilB-GFP
SurG-GFP
PilA-GFP
PilB-GFP
SurG-GFP
80 kDa
70 kDa
48 kDa
27 kDa

Figure 4

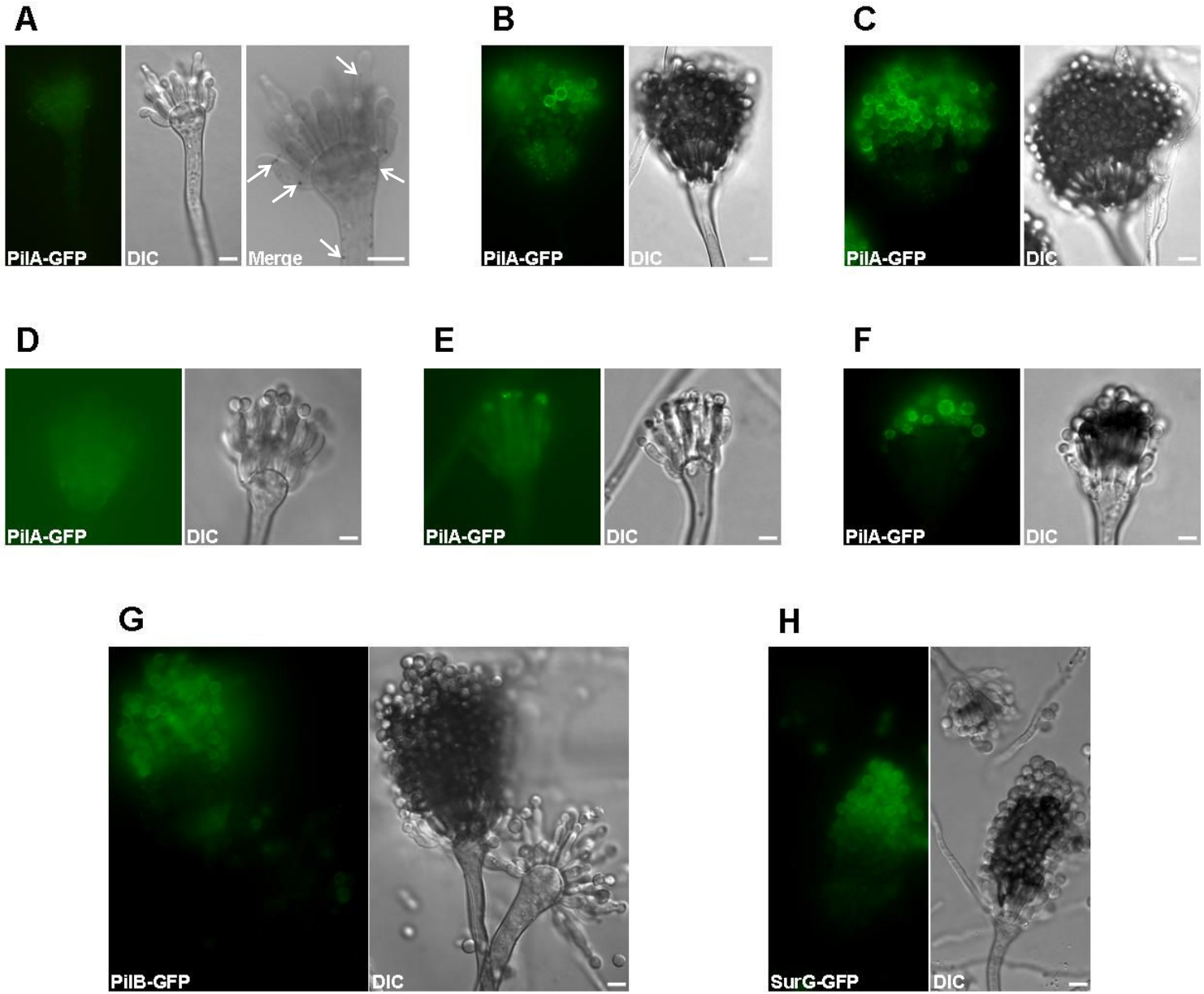
A
PilA-GFP
DIC
Merge
B
PilA-GFP
DIC
C
PilA-GFP
DIC
D
PilA-GFP
DIC
E
PilA-GFP
DIC
F
PilA-GFP
DIC
G
PilB-GFP
DIC
H
SurG-GFP
DIC

Figure 5

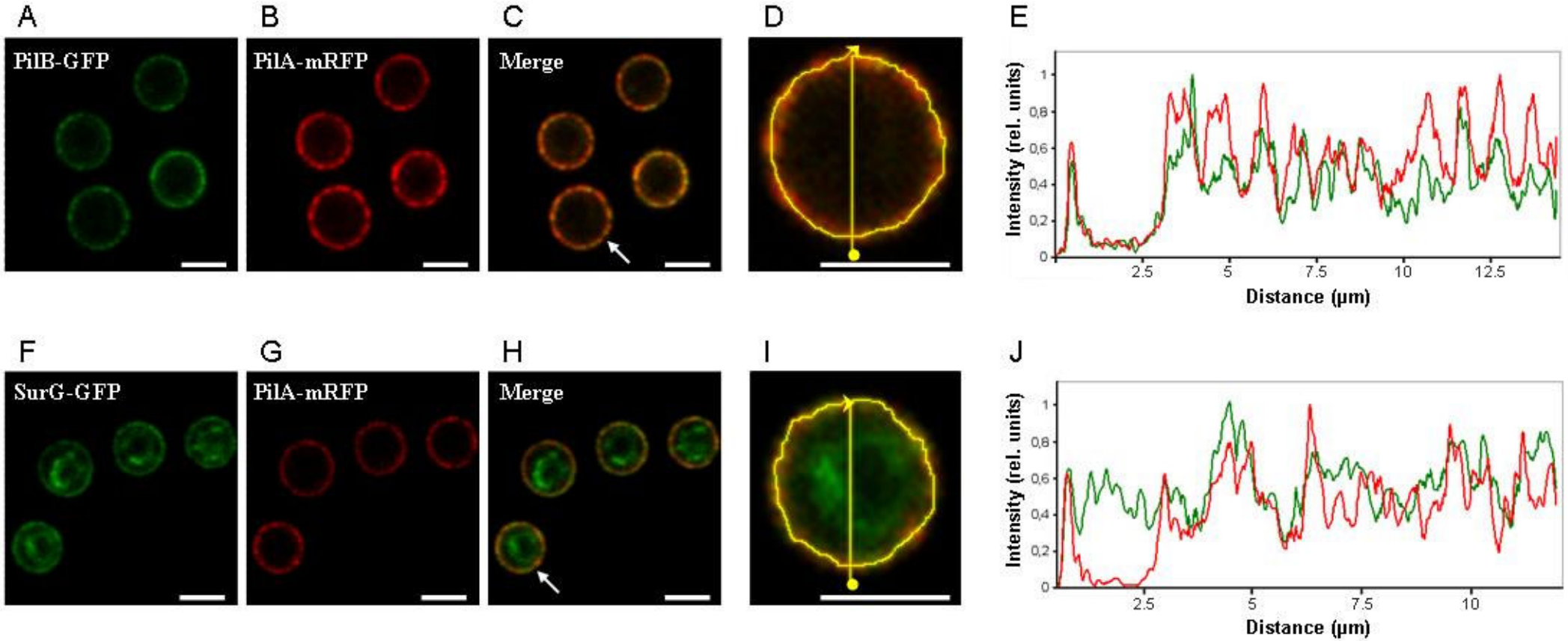
A
PilB-GFP
B
PilA-mRFP
C
Merge
D
E
Intensity (rel. units)
0
0,2
0,4
0,6
0,8
1
2.5
5
7.5
10
12.5
Distance (µm)
F
SurG-GFP
G
PilA-mRFP
H
Merge
I
J
Intensity (rel. units)
0
0,2
0,4
0,6
0,8
1
2.5
5
7.5
10
Distance (µm)

Figure 6

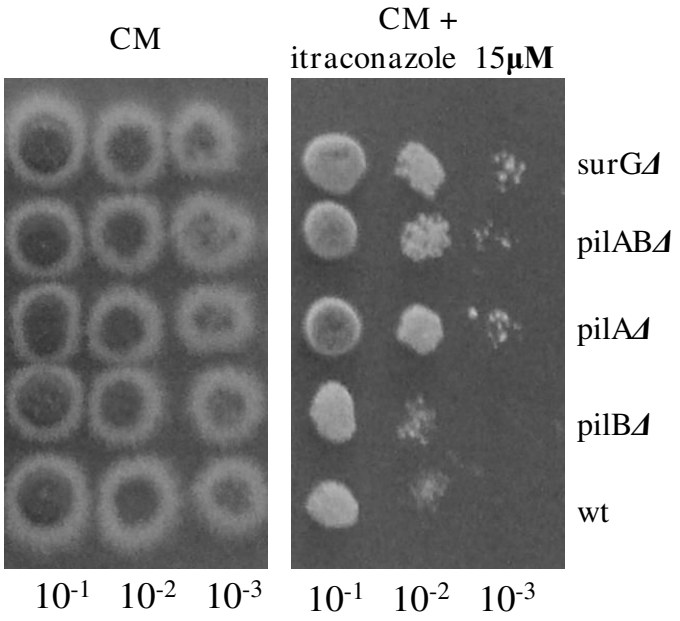
CM
CM +
itraconazole 15μM
surGΔ
pilABΔ
pilAΔ
pilBΔ
wt
10-1 10-2 10-3
10-1 10-2 10-3

Figure 7

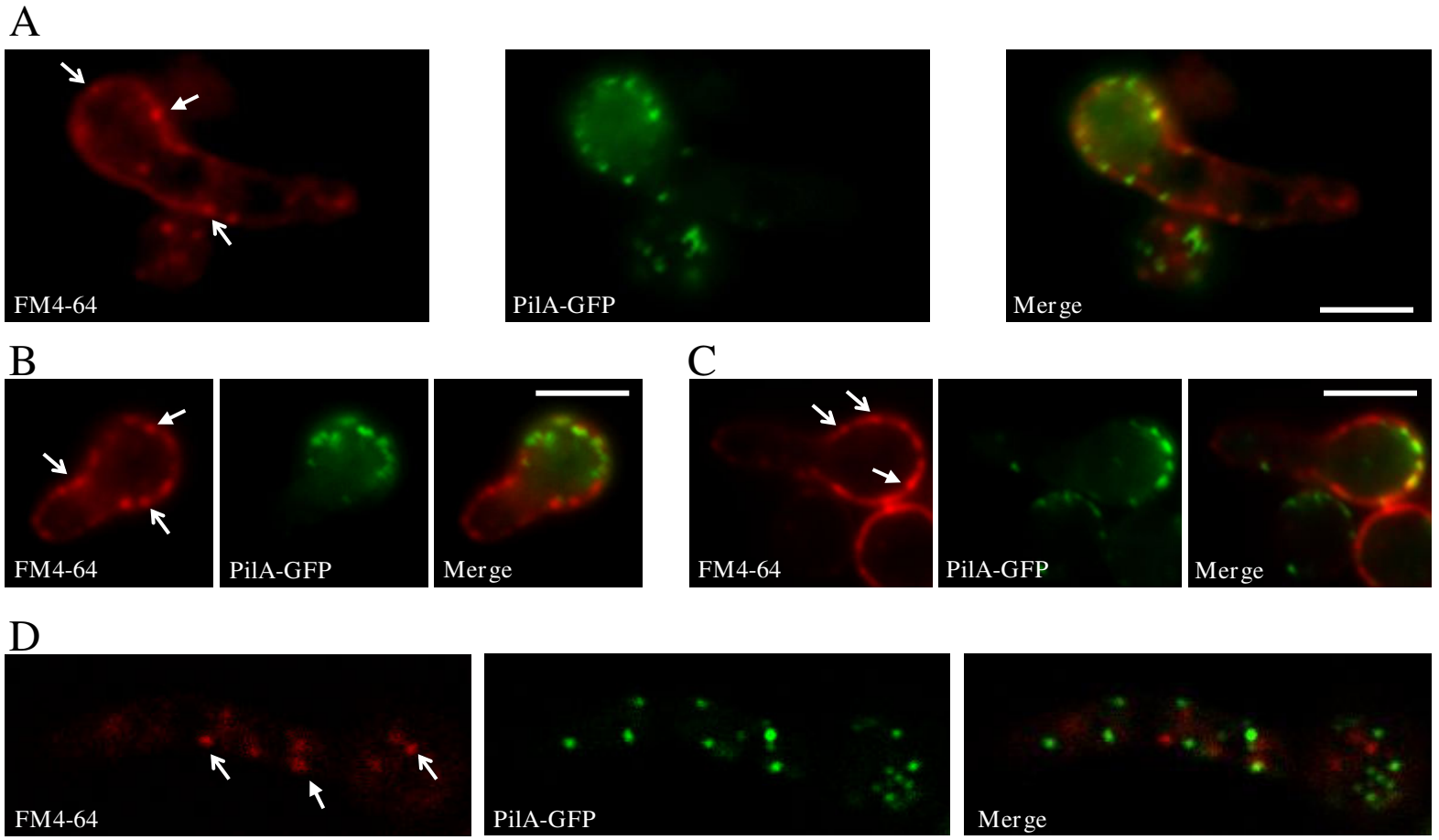
A
FM4-64
PilA-GFP
Merge
B
FM4-64
PilA-GFP
Merge
C
FM4-64
PilA-GFP
Merge
D
FM4-64
PilA-GFP
Merge

Figure 8

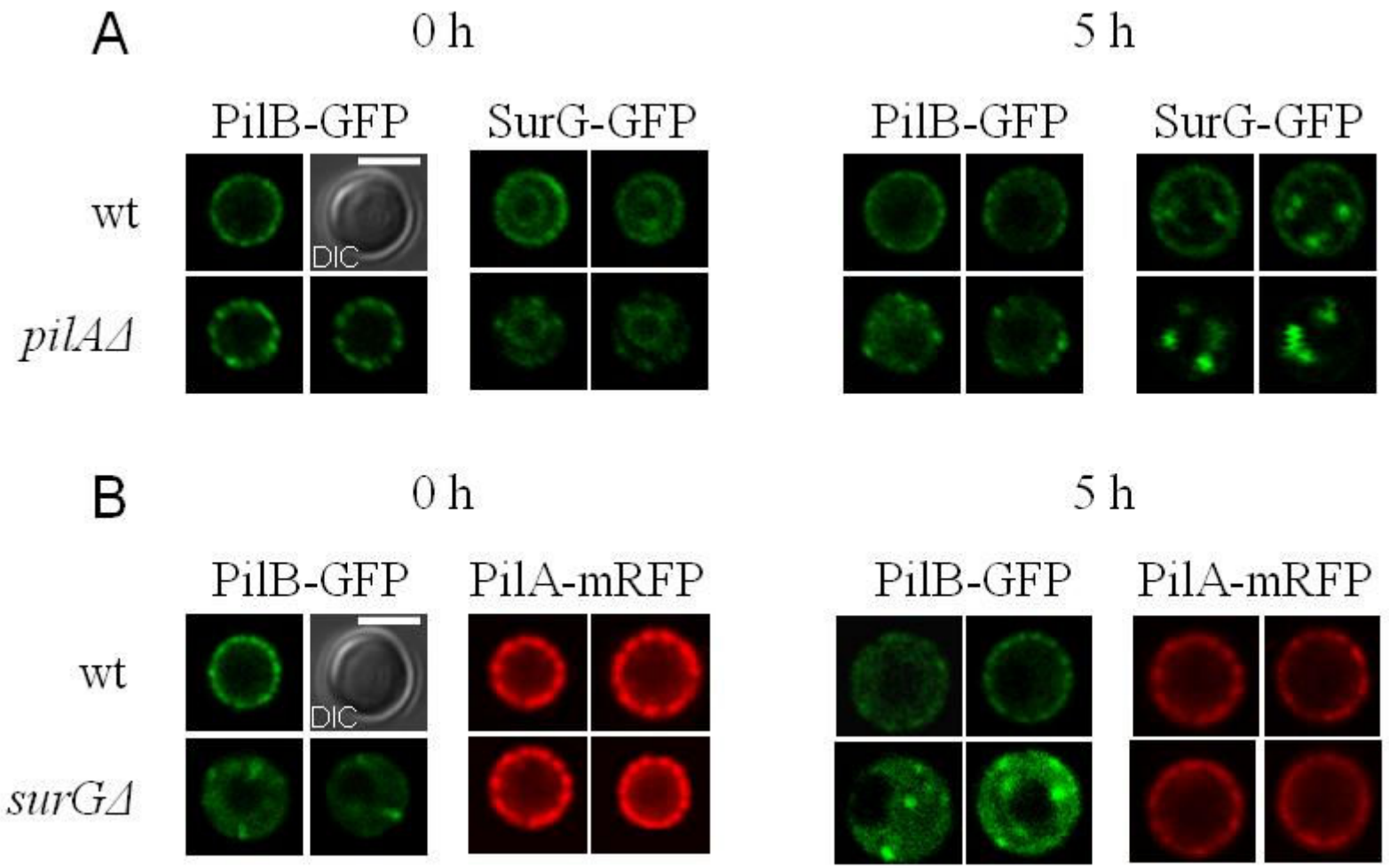
A
0 h
5 h
PilB-GFP
SurG-GFP
PilB-GFP
SurG-GFP
wt
pilAΔ
DIC
B
0 h
5 h
PilB-GFP
PilA-mRFP
PilB-GFP
PilA-mRFP
wt
surGΔ
DIC

Figure 9

Table 1

***Aspergillus nidulans* strains used in this study**

Strains	Genotypes	Reference
wt (1)	*pabaA1*	CS2498 (Fungal Genetics Stock Center)
nkuAΔ pyrG89 riboB2	*pyrG89;argB2;nkuAΔ::argB*$^{+}$ *pabaB22;riboB2*	(provided by Dr. M. Peñalva)
nkuAΔ pyrG89 pyroA4	*pyrG89;argB2;nkuAΔ::argB*$^{+}$ *pyroA4*	(provided by Dr. M. Peñalva)
LO1516	*pyrG89;argB2;nkuAΔ::argB*$^{+}$ *pyroA4;hhoA::mrfp::Afribo;riboB2*	(provided by Prof. C. Scazzocchio)
VS79	*pyrG89;argB2;nkuAΔ::argB*$^{+}$ *pabaB22;pilA::sgfp::AfpyrG*$^{+}$*;riboB2*	This study
VS80	*pyrG89;pilB::sgfp::AfpyrG*$^{+}$*;argB2;nkuAΔ::argB*$^{+}$ *pabaB22;riboB2*	This study
VS81	*pyrG89;surG::sgfp::AfpyrG*$^{+}$*argB2;nkuAΔ::argB*$^{+}$ *pabaB22;riboB2*	This study
VS83	*pyrG89;argB2;nkuAΔ::argB*$^{+}$ *pyroA4;pilA::mrfp::AfpyrG*$^{+}$	This study
VS84	*pyrG89;argB2 surGΔ::Afpyro*$^{+}$*;nkuAΔ::argB*$^{+}$ *pyroA4*	This study
VS85	*pyrG89;pilBΔ::AfpyrG*$^{+}$*;argB2;nkuAΔ::argB*$^{+}$ *pabaB22;riboB2*	This study
VS86	*pyrG89;argB2;nkuAΔ::argB*$^{+}$ *pabaB22 pilAΔ::Afribo*$^{+}$*;riboB2*	This study
VS87	*pyrG89;pilBΔ::AfpyrG*$^{+}$*;argB2;nkuAΔ::argB*$^{+}$ *pabaB22;pilAΔ::Afribo*$^{+}$*;riboB2*	This study
VS91	*pyrG89;argB2 surG::sgfp::AfpyrG*$^{+}$*;nkuAΔ::argB*$^{+}$*;pilA::mrfp::AfpyrG*$^{+}$*;riboB2*	This study
VS94	*pyrG89;pilB::sgfp::AfpyrG*$^{+}$*;argB2;nkuAΔ::argB*$^{+}$*;pilA::mrfp::AfpyrG*$^{+}$*;riboB2*	This study

VS118	*pyrG89;argB2 surGΔ::Afpyro^{+};nkuAΔ::argB^{+} pyroA4;pilA::mrfp::AfpyrG^{+}*	This study
VS125	*agtA::sgfp::AfpyrG^{+};argB2;riboB2*	This study
VS128	*pyrG89;pilB::sgfp::AfpyrG^{+};argB2;nkuAΔ::argB^{+} pabaB22;pilAΔ::Afribo^{+};riboB2*	This study
VS129	*pyrG89;surG::sgfp::AfpyrG^{+}argB2;nkuAΔ::argB^{+} pabaB22;pilAΔ::Afribo^{+};riboB2*	This study
VS132	*pyrG89;pilB::sgfp::AfpyrG^{+};argB2 surGΔ::Afpyro^{+};nkuAΔ::argB^{+} pyroA4*	This study
VS145	*pyrG89;surG::sgfp::AfpyrG^{+}argB2;nkuAΔ::argB^{+} pabaB22;hhoA::mrfp::Afribo^{+};riboB2*	This study
VS153	*pyrG89;pilB::sgfp::AfpyrG^{+};argB2;nkuAΔ::argB^{+} pyroA4;hhoA::mrfp::Afribo^{+};riboB2*	This study
VS172	*pyrG89 agtA::sgfp::AfpyrG^{+};argB2;nkuAΔ::argB^{+};pilAΔ::Afribo^{+};riboB2*	This study
VS186	*yA2; pantoB100, prnB::sgfp::trpC* C*-term;pyrG89;argB2; nkuAΔ::;pilA::mrfp::AfpyrG^{+}*	This study

Table 2

Plasmids used in this work

Cloning vector	Description	Reference
pRG3	pGEM:*18SrRNA*	Delcasso-Tremousaygue *et al.,* (1988)
p1548	*AfriboB*	Szewczyk *et al.,* 2006 (provided by Dr. M. Peñalva).
p1547	*AfpyroA*	Szewczyk *et al.,* 2006 (provided by Dr. M. Peñalva).
p1439	5GA:*sgfp:AfpyrG*	Szewczyk *et al.,* 2006 (provided by Dr. M. Peñalva).
p1491	5GA:*smrfp:AfpyrG*	Szewczyk *et al.*, 2006 (provided by Dr. M. Peñalva).

Table 3

Oligonucleotides used in this study

Name	Sequence 5′ → 3′
PilAΔ-Ribo F	GCA GAA TAT CGG CTG GTC TC CGC TCT AGA ACT AGT GGA TCC
PilAΔ-Ribo R	GCT CAT TCA GTG AGT GCT CG CCT CGA GGT CGA CGG TAT CG
PilBΔ-PyrG F	CAC CTG TCT AGC CTC AGC AA GTC GCC TCA AAC AAT GCT CTT C
PilBΔ-PyrG R	CAC AAA GCA CTA ATC ACC CCT T CTG AGA GGA GGC ACT GAT GC
SurGΔ-Pyro F	GTC TAC TCG TCT CTC ATC AGA CGC TCT AGA ACT AGT GGA TCC
SurGΔ-Pyro R.	GTG TAT AGC CGA CAG CAG CA CCT CGA GGT CGA CGG TAT CG
P1 PilAΔ	CGA TCC TAG CTC TCA GGA TC
P3 PilAΔ	GGA TCC ACT AGT TCT AGA GCG GAG ACC AGC CGA TAT TCT GC
P4 PilAΔ	CGA TAC CGT CGA CCT CGA GG CGA GCA CTC ACT GAA TGA GC
P6 PilAΔ	ACC AAC CTA GTC GAC GTG AC
P1 PilBΔ	CTC AGC TGA GAG ACT GTC AG
P3 PilBΔ	GAA GAG CAT TGT TTG AGG CGA C TTG CTG AGG CTA GAC AGG TG
P4 PilBΔ	GCA TCA GTG CCT CCT CTC AG AAG GGG TGA TTA GTG CTT TGT G
P6 PilBΔ	TCG GAG TCA ATG TAG TAC AGC
P1 SurGΔ	GCT CAC ATC CAC AAT GTC TAG
P3 SurGΔ	GGA TCC ACT AGT TCT AGA GCG TCT GAT GAG AGA CGA GTA GAC
P4 SurGΔ	CGA TAC CGT CGA CCT CGA GG TGC TGC TGT CGG CTA TAC AC
P6 SurGΔ	GAC TGC CAC ACC TCA CCT C
P2 PilAΔ	GCT GAA CCA GAA GAG GCT GC
P5 PilAΔ	GCA TCC ATG ATG TCA GCA TAC
P2 PilBΔ	TCA TCA CCA GGC AAG ATC ATC
P5 PilBΔ	CAT CGT TCC CAT GCT CAG AC

P2 SurGΔ	TCT TGT GCT GAG GGA ACT AAG
P5 SurGΔ	CGT CCT CAT CCG TGT CTG C
PilA F	CGG GAG CCT GTC CCT GTC GGA GCT GGT GCA GGC GCT G
PilA R	GCT CAT TCA GTG AGT GCT CG CTG AGA GGA GGC ACT GAT GC
PilA P1	GCA TCG TAC ATA CTC TAT GCG
PilA P2	CAC CAC TCT CCT CGA CCA AG
PilA P3	CAG CGC CTG CAC CAG CTC C GAC AGG GAC AGG CTC CCG
PilA P4	GCA TCA GTG CCT CCT CTC AG CGA GCA CTC ACT GAA TGA GC
PilA P5	GCA TCC ATG ATG TCA GCA TAC
PilA P6	ACC AAC CTA GTC GAC GTG AC
PilB F	AGC GAG TTG CAG TGC CCA TT GGA GCT GGT GCA GGC GCT G
PilB R	CAC AAA GCA CTA ATC ACC CCT T CTG AGA GGA GGC ACT GAT GC
PilB P1	GCA GAA GAA GGA GCT CTG TC
PilB P2	CGT GCT GAT GGC AGA AAT GG
PilB P3	CAG CGC CTG CAC CAG CTC C AAT GGG CAC TGC AAC TCG CT
PilB P4	GCA TCA GTG CCT CCT CTC AG AAG GGG TGA TTA GTG CTT TGT G
PilB P5	CAT CGT TCC CAT GCT CAG AC
PilB P6	TCG GAG TCA ATG TAG TAC AGC
SurG F	GCA ACA AGG AAA TCG CTC CCG GAG CTG GTGCAG GCG CTG GAG
SurG R	GTG TAT AGC CGA CAG CAG CAC TGA GAG GAG GCA CTG ATG CGT G
SurG P1	CTT CAT CGT TCA AGC TTC AGG
SurG P2	TCT ACT CGT CTC TCA TCA GAG
SurG P3	C TCC AGC GCC TGC ACC AGC TCC GGG AGC GAT TTC CTT GTT GC
SurG P4	CAC GCA TCA GTG CCT CCT CTC AG TGC TGC TGT CGG CTA TAC AC
SurG P5	TGT CGA GTT TCT GCC TCT CC
SurG P6	GAC TGC CAC ACC TCA CCT C